© The Authors. CC BY 4.0 Int. Licencee: SV-JME

Coaxial Monitoring of Meltpool for Laser Powder Bed Fusion Process Control

Dominik Kozjek[1,✉] – Drago Bračun[1] – Andrej Jeromen[1] – Fred M. Carter III[2] – Primož Podržaj[1] – Edvard Govekar[1]

1 University of Ljubljana, Faculty of Mechanical Engineering, Slovenia
2 DMG MORI Advanced Manufacturing Innovation Center, USA

✉ dominik.kozjek@fs.uni-lj.si

Abstract *Reliable process monitoring is critical for advancing laser powder bed fusion of metals (PBF-LB/M), as it provides the process information required for corrective control actions to prevent defects such as lack-of-fusion and keyhole porosity. A promising approach for PBF-LB/M process monitoring is coaxial measurement of light emitted from the meltpool area. More than two hundred research studies on coaxial monitoring of the meltpool have been performed, but there is still no validated and reliable method for measuring a suitable variable that could be directly used as an input for high-resolution control of the PBF-LB/M process, enabling process parameters such as laser power and scan speed to be dynamically adjusted not only at the part level, but locally for individual micrometer-scale segments along the scan track. This work reviews existing research studies on coaxial meltpool monitoring and identifies potential future research and development directions toward a standard and reliable meltpool monitoring method. Meltpool depth is identified as a particularly promising control-relevant variable. With the ability to monitor and control meltpool depth, it is possible to avoid undesirable process conditions due to too high or too low energy input, which would result in defects like keyhole porosity or lack-of-fusion. However, only five studies have attempted to estimate the melt pool depth coaxially during the PBF-LB/M process. Despite these attempts, there is no sufficiently validated method for high-resolution coaxial monitoring of meltpool depth in PBF-LB/M. The potential solution seems to be in combining concepts and recent discoveries from two-color coaxial camera- and photodiode-based meltpool area monitoring approaches. Based on the existing literature and hands-on experiences with establishing and working with coaxial monitoring systems, this work also provides guidelines and lists the most common challenges for implementing coaxial monitoring of the meltpool in the PBF-LB/M process.*

Keywords *PBF-LB/M process, SLM, coaxial monitoring, meltpool, light emission, wavelength, review*

Highlights

- *Review of more than 200 studies on coaxial meltpool monitoring in PBF-LB/M.*
- *Meltpool depth is an important variable for process control.*
- *Two-color camera-based coaxial monitoring shows promise for estimating meltpool depth.*
- *Key implementation challenges and guidelines for coaxial monitoring are presented.*

1 INTRODUCTION

In the laser powder bed fusion of metals (PBF-LB/M), a laser beam selectively melts a thin layer of metal powder in a powder bed (Fig. 1). The layer thickness is typically 20 µm to 60 µm, depending on the material and process. The process of melting the powder with a laser beam is carried out layer by layer. In each layer, the process involves spreading a thin layer of metal powder on the build platform and then melting it using a focused laser beam. After the solidification of a melted layer, the build platform descends, and the next layer of powder is spread and selectively melted above the previously solidified layer. The main input process parameters in PBF-LB/M are laser power, scanning speed, layer thickness, and scan pattern, which defines the laser beam path within each layer. Conventional PBF-LB/M scan strategies typically employ constant laser power and scan speed along individual scan vectors. However, because the local thermal conditions vary continuously as a function of geometry, scan history, heat accumulation, and proximity to boundaries, constant process parameters result in spatial variations of the meltpool geometry and temperature. Recent studies have therefore investigated spatially and temporally varying laser power and/or scan speed to compensate for these variations [1-9]. Modern laser/scanner control hardware permits such modulation on microsecond timescales, corresponding to spatial intervals on the order of tens of micrometers, or potentially less, at typical PBF-LB/M scan speeds. Such advanced control approaches can be enabled by high-resolution in-situ monitoring of process conditions.

There are several ways to monitor melting process conditions in situ during the PBF-LB/M process. One of the more accurate and reliable approaches is to coaxially measure light emissions from the meltpool area. In a typical PBF-LB/M system, the laser beam travels from the laser source through the galvoscanner, which then directs the laser beam to a target position on the powder bed (Fig. 2). Before the laser beam hits the powder bed, the laser beam also travels through the F-theta lens, which ensures that the laser beam is properly focused on the flat powder bed surface in all positions on the horizontal plane. The term coaxial measurement means that light emissions from the meltpool and its surroundings travel back through the same optical path as the laser beam. Using beam splitters, the emitted light signal is directed away from the optical path after it travels back through the galvoscanner. The light emitted from the meltpool is received by the optical sensor, which is typically a camera or a photodiode. Additionally, just before the intensity of the light emission signal is measured by the photodiode or camera, the emitted light can be split into two or more beams, and each of these beams can be filtered to a different wavelength band and measured with an individual sensor for each of these parts of the emitted light. This work presents findings and gives future research directions based on

the review of existing research studies on coaxial monitoring of the meltpool in PBF-LB/M.

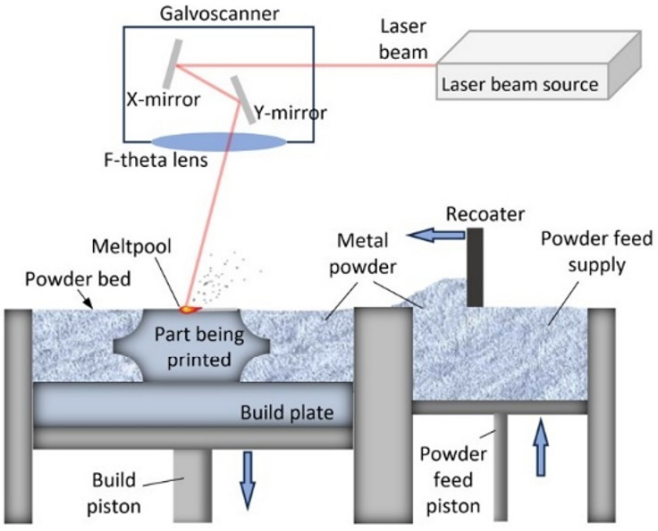


Fig. 1. Laser powder bed fusion of metals

Although several process signatures can be exploited for in-situ monitoring of PBF-LB/M, including spatter, plume emissions, acoustic emissions, and powder-bed characteristics [10–13], the present work focuses on the meltpool because it represents the immediate region in which laser energy is converted into melting and subsequent material consolidation [10–13]. Consequently, variations in meltpool geometry, temperature, and dynamics are closely associated with changes in the local energy balance and with defect-forming mechanisms such as insufficient fusion, unstable keyhole formation, and balling [12–14]. In particular, insufficient meltpool penetration or overlap can promote lack-of-fusion defects, whereas excessive energy input and unstable deep meltpools are associated with keyhole-induced porosity [13]. Previous studies have therefore identified meltpool characteristics as informative process signatures for assessing local process stability and predicting internal flaws [13].

Meltpool monitoring is also attractive from a process-control perspective because the measured signal originates at the location of the laser–material interaction and can be acquired with high spatial and temporal resolution [10,11]. In a coaxial configuration, the sensing field of view follows the processing laser, providing inherent spatial correspondence between the monitored signal and the instantaneous processing location [10]. Other signatures, such as spatter, plume, and acoustic emissions, provide important complementary information and may improve defect classification when combined with meltpool measurements [11–13]; however, they generally represent secondary phenomena generated by the underlying laser–meltpool interaction. For these reasons, and because the objective of the present work is ultimately directed toward local, spatially resolved process monitoring and control, the meltpool was selected as the primary process signature.

Although both coaxial and off-axis configurations are widely employed for in-situ monitoring of PBF-LB/M, they provide different perspectives on the process [13,15]. Off-axis optical and thermal imaging generally offer greater flexibility in sensor selection and field of view, enabling observation of the meltpool together with surrounding phenomena such as spatter, plume behavior, and the thermal evolution of the build surface [11,13,15]. Acoustic sensing provides complementary information on process dynamics without requiring direct optical access [13,15]. These techniques are therefore highly valuable for process understanding and, particularly in multimodal monitoring configurations, can provide information complementary to coaxial optical sensing [11,13,15]. However, off-axis sensing does not provide the same inherent spatial registration between the sensor field of view and the rapidly moving laser–material interaction zone as coaxial optical sensing [10].

In a coaxial configuration, process radiation is collected along, or close to, the optical axis of the processing laser, such that the monitored region follows the laser as it scans across the build plane [10]. This inherent spatial coordination is particularly advantageous in PBF-LB/M, where the meltpool is typically only tens to hundreds of micrometers in size and evolves on microsecond timescales [10]. Coaxial sensing therefore enables high-speed, meltpool-scale measurements that can be directly associated with the instantaneous laser position, facilitating the reconstruction of spatially resolved process information and its potential integration with machine control [10,15]. Importantly, these advantages do not imply that coaxial monitoring is universally more accurate or informative than off-axis, acoustic, or multimodal approaches; rather, coaxial monitoring offers a distinctive combination of inherent spatial registration with the laser, high temporal resolution, and suitability for integration with real-time process monitoring and feedback strategies [10,15]. It is this combination, together with the increasing interest in spatially

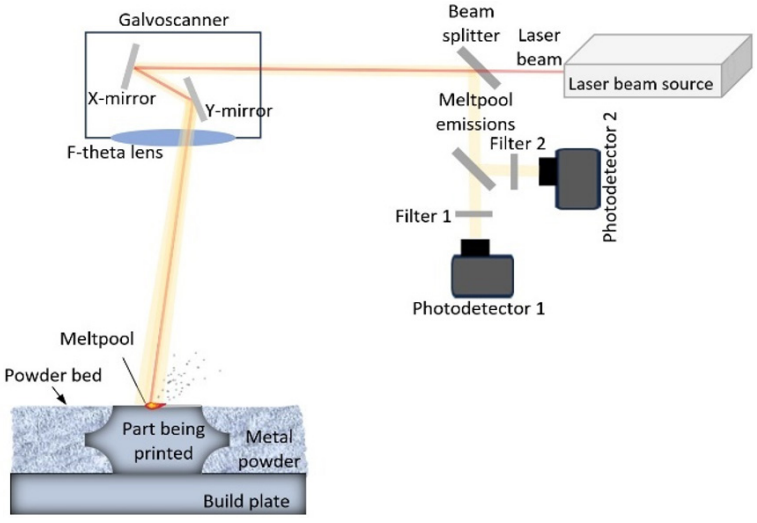


Fig. 2. Typical coaxial monitoring system

resolved in-situ monitoring and closed-loop control of PBF-LB/M, that motivates the specific focus of the present review on coaxial meltpool monitoring [10,15].

Previous reviews of in-situ monitoring in PBF-LB/M, namely McCann et al. [16], Grasso et al. [17], Hou et al. [18], Cai et al. [19], Chen et al. [20], and Papatheodorou et al. [21], have provided broad surveys of sensing modalities, process signatures, defect-detection approaches, and process-control strategies. In contrast, the present review focuses specifically on coaxial optical monitoring of the meltpool from the perspective of its suitability for high-resolution process control. By systematically analyzing more than 200 published studies, the review provides a comparison of coaxial monitoring systems in terms of sensor type, measurement wavelength, acquisition frequency, two-color pyrometry, estimated meltpool characteristics, and demonstrated use for process control. Beyond cataloguing existing approaches, the review critically examines which measured variables can provide sufficiently robust information for corrective control actions and identifies meltpool depth as a particularly promising control variable for distinguishing process conditions associated with lack-of-fusion and keyhole porosity. The limited existing approaches for coaxial meltpool depth estimation are therefore examined, revealing important limitations in their applicability, temporal resolution, validation across processing conditions, and transferability between materials. Based on this analysis, the combination of spatially resolved coaxial camera measurements with two-color pyrometry is identified as a promising direction toward reliable, high-resolution meltpool-depth monitoring. Finally, the review complements the scientific literature with practical guidelines and implementation challenges for coaxial monitoring systems, thereby providing both a consolidated reference for the current state of the field and a roadmap toward standardized, control-oriented coaxial meltpool monitoring in PBF-LB/M.

1.1 Literature Search and Review Methodology

A structured literature search was conducted to identify relevant studies concerning coaxial monitoring of the meltpool in laser powder bed fusion of metals (PBF-LB/M). Google Scholar was used as the primary literature search engine because of its broad coverage of journal articles, conference proceedings, and other scientific publications relevant to additive manufacturing and process monitoring. The search was performed using combinations of terminology describing the manufacturing process, coaxial monitoring configuration, and sensing or measurement technology. The principal search expression was: "((laser powder bed fusion) OR LPBF OR L-PBF OR PBF OR PBF-LB/M OR (selective laser melting) OR SLM) AND (coaxial OR co-axial OR on-axis) AND (camera OR photodiode OR photodiodes OR sensor OR pyrometer OR measurement OR measurements)".

The terminology related to the manufacturing process intentionally includes both current and historically used nomenclature (e.g., PBF-LB/M, LPBF, L-PBF, SLM, and selective laser melting) to account for changes in terminology within the literature and thereby minimize the omission of relevant earlier studies. Similarly, several terms describing the optical configuration (coaxial, co-axial, and on-axis) and sensing technologies were included to capture variations in terminology among different research groups.

The initial search results were screened for relevance to coaxial sensing and monitoring of the meltpool region during PBF-LB/M. Particular attention was given to studies employing optical sensing approaches such as cameras, photodiodes, and pyrometric systems, as well as studies addressing the acquisition, interpretation, or application of coaxially collected process signals. Publications that did not concern PBF-LB/M, did not employ a coaxial/on-axis monitoring configuration, or were not relevant to melt-pool/process monitoring were excluded from the core literature considered in this review work.

The database search was complemented by backward and forward literature exploration. In particular, the reference lists and related-work discussions of relevant publications were examined to identify additional studies that were not readily retrieved by the initial keyword search. Relevant publications identified through this citation-based approach were subsequently evaluated according to the same topical criteria. This iterative procedure continued until the newly examined publications predominantly referred to studies that had already been identified or did not provide additional relevant contributions.

The resulting body of literature was then reviewed and organized according to the principal coaxial sensing approaches, measurement configurations, monitored process characteristics, and reported applications. The objective of this methodology was not to perform a formal systematic review or meta-analysis, but rather to provide a structured and sufficiently comprehensive assessment of the development, capabilities, and limitations of coaxial meltpool monitoring approaches reported for PBF-LB/M.

2 COAXIAL MONITORING OF MELTPOOL IN PBF-LB/M

Table 1 summarizes research related to coaxial monitoring of the meltpool for PBF-LB/M. It indicates whether coaxial monitoring was used for process control and summarizes the sensor types, measurement wavelength bands and frequencies, application of two-color pyrometry, and estimation of meltpool temperature, depth, and other meltpool characteristics. In total, more than 200 research studies with in-situ coaxial monitoring systems were performed. The research group/institution listed in the first column of Table 1 corresponds to the affiliation of the first author of each publication. In some cases where the main experimental equipment is recognized to belong to a specific research institution (which may not be of the first authors), and coauthors from that institution are collaborating in the research study, the published work is also categorized under this institution. It should be noted that many of the listed publications involve collaborations with researchers from more than just one institution.

One of the most active research groups in terms of the number of published works in the field of coaxial measurement in PBF-LB/M is the group at the National Institute of Standards and Technology (NIST) in the United States (see the first item in Table 1). Their research focuses on camera-based coaxial measurement of the PBF-LB/M process conditions. They also carried out foundational work for the photodiode-based coaxial measuring systems. Another active research group is at the Polytechnic University of Milan. In most of their research work, they investigated camera-based coaxial measurement systems. The third active research group is at Northwestern University in the United States. Their research focuses on single- and two-color photodiode-based coaxial measurements. Besides the three groups mentioned above, there are several other research groups that are actively researching in the field of coaxial monitoring of the PBF-LB/M process. For example, some of them are at KU Leuven, University of Pittsburgh, University College Dublin, ETH Zürich, and Imperial College London. Their research includes camera, photodiode or both, as well as other type (e.g., spectrometer-based) coaxial measuring systems for PBF-LB/M. Table 1 systematically summarizes characteristics and published works from individual research groups that have investigated coaxial monitoring in PBF-LB/M. The table provides an comprehensive list

Table 1. Coaxial-measurement-based monitoring systems in PBF-LB/M

Research group*	Used for control	Coaxial camera	Coaxial photodiode	Other coaxial sensors	Wavelengths c – camera p – photodiode py – pyrometer s – spectrometer o – other / - not specified or not found	Measuring frequency c – camera p – photodiode py – pyrometer s – spectrometer o – other / - not specified or not found	Two-color pyrometry	Temperature estimation	Meltpool depth estimation	Other meltpool dimensions est.	Publications
NIST – National Institute of Standards and Technology (U.S.)	•	•	•		850±20 nm (c) 580±5 nm (p) 520±20 nm (p)	100 kHz (p) 30 kHz (c) 20 kHz (c) 10 kHz (c) 2 kHz (c)		•		•	Lane et al., 2016 [22]; Lane et al., 2017 [23]; Fox et al., 2017 [24]; Yeung et al., 2018 [25]; Yeung et al., 2019 [2]; Yang et al., 2020 [26]; Lane et al., 2020 [27]; Lane et al., 2020 [28]; Yeung & Lane, 2020 [4]; Lane & Yeung, 2020 [29]; Yeung et al., 2020 [30]; Feng et al., 2020 [31]; Feng et al., 2020 [32]; Lu et al., 2020 [33]; Yang et al., 2021 [34]; Kim et al., 2021 [35]; Yang et al., 2022 [36]; Fathizadan et al., 2023 [37]; Liu X. et al., 2024 [38]; Chen H. et al., 2024 [39]; Kim et al., 2025 [40]; Hong et al., 2024 [41]; Yang et al., 2024 [42]; Yeung, 2025 [9]; Yang et al., 2025 [43]; Hong et al., 2025 [44]
Polytechnic University of Milan	•	•	•	•	1450-1700 nm (py1) 2000-2500 nm (py2) 1100-1700 nm (p) 1064±10 nm (c) 850-1000 nm (c) 700-1000 nm (c) 670 nm (c) 640 nm (c) 550-950 nm (p) 350-700 nm (c) visible (c, p)	100 kHz (py) 100 kHz (p) 6.4 kHz (c) 1.2 kHz (c) 0.068 kHz (c)			•	•	Bozzani & Beretta, 2015 [45]; Demir et al., 2018 [46]; Bejan, 2018 [47]; Vasileska, 2019 [48]; Mazzoleni et al., 2019 [49]; Mazzoleni et al., 2019 [50]; Pacher et al., 2019 [51]; Demir et al., 2019 [52]; Vasileska et al., 2020 [53]; Caprio et al., 2022 [54]; Vasileska et al., 2022 [55]; Gronle et al., 2023 [56]; Cacace et al., 2025 [57]
Northwestern University	•		•		700±5 nm, 680±5 nm, 400-900 nm	200 kHz 100 kHz	•	•	•		Kozjek et al., 2022 [58]; Porter et al., 2022 [59]; Kozjek et al., 2023 [3]; Kozjek et al., 2023 [60]; Carter et al., 2023 [61]; Carter et al., 2024 [5]; Liao et al., 2024 [62]; Kozjek et al., 2024 [63]; Samaei et al., 2024 [64]; Meng et al., 2025 [65]
KU Leuven	•	•	•		850-950 nm 780-900 nm	20 kHz, 10 kHz (c) 1.2 kHz			•	•	Kruth et al., 2007 [66]; Berumen et al., 2010 [67]; Craeghs et al., 2010 [68]; Clijsters et al., 2014 [69]; Goossens & Van Hooreweder, 2021 [70]; Thanki et al., 2022 [71]; Tao et al., 2023 [72]; Thanki et al., 2024 [73]; Tao et al., 2024 [74]
University of Pittsburgh		•			620±10 nm 620 nm 550 nm	30 kHz 25 kHz 22.5 kHz 20 kHz	•	•	•	•	Vallabh & Zhao, 2022 [75]; Vallabh et al., 2022 [76]; Vallabh et al., 2022 [77]; Zhang et al., 2022 [78]; Vallabh & Zhao, 2023 [79]; Zhao et al., 2024 [80]; Akhavan et al., 2024 [81]; Alam et al., 2025 [82]
Nanjing University of Science and Technology		•	•		600–900 nm (p) 830-900 nm (c) 600±100 nm (c)	100 kHz (p) 10 kHz (c)				•	Zou et al., 2024 [83]; Li et al., 2026 [84]; Li et al., 2025 [85]; Li et al., 2025 [86]; Zou et al., 2025 [87]
University of Waterloo			•		750-900 nm visible-NIR	60 kHz 59 kHz					Taherkhani et al., 2021 [88]; Taherkhani et al., 2022 [89]; Taherkhani, 2022 [90]; Taherkhani et al., 2023 [91]; Liravi et al., 2024 [92]; Toorandaz et al., 2024 [93]
Imperial College London		•			950 nm 700 nm	100 kHz 20 kHz	•	•		•	Hooper, 2018 [94]; de Winton et al., 2021 [95]; Gaikwad et al., 2022 [12]; Larsen & Hooper, 2023 [96]; Taylor et al., 2025 [97]
Rensselaer Polytechnic Institute	•	•			880±35 nm 800-950 nm NIR	3.5 kHz 2 kHz 0.8 kHz				•	Shkoruta et al., 2019 [98]; Shkoruta et al., 2020 [99]; Park et al., 2022 [100]; Shkoruta et al., 2022 [101]; Park et al., 2024 [102];
University College Dublin			•		IR Visible UV	100 kHz					Egan & Dowling, 2019 [103]; Egan et al., 2020 [104]; Egan & Dowling, 2020 [105]; Keaveney et al., 2020 [106]; Power et al., 2024 [107]
Wuhan Textile University; Huazhong University of Science and Technology		•			/	10 kHz				•	Cao et al., 2023 [108]; Cao et al., 2025 [109]; Cao et al., 2024 [110]; Zhang et al., 2024 [111]

Research group*	Used for control	Coaxial camera	Coaxial photodiode	Other coaxial sensors	Wavelengths c – camera p – photodiode py – pyrometer s – spectrometer o – other / - not specified or not found	Measuring frequency c – camera p – photodiode py – pyrometer s – spectrometer o – other / - not specified or not found	Two-color pyrometry	Temperature estimation	Meltpool depth estimation	Other meltpool dimensions est.	Publications
University of Liverpool			•		1100-2000 nm 1100-1700 nm 1080-1700 nm 700-1050 nm 300-1000 nm	100 kHz					Okaro et al., 2019 [112]; Jayasinghe, 2022 [113]; Jayasinghe et al., 2022 [114]; Villalva, 2024 [115]
ETH Zürich	•	•	•	•	1650-1800 nm (p) 1500-1700 nm (py) 1450-1800 nm (p) 1450-1650 nm (p) 850 nm (c)	100 kHz (p) 100 kHz (py) 12.5 kHz (c) 2.5 kHz (p) 2 kHz (p)	•	•	•		Gutknecht et al., 2020 [116]; Gutknecht et al., 2021 [1]; Gutknecht et al., 2021 [117]; Kavas et al., 2025 [118]
Lawrence Livermore National Laboratory		•	•	•	1600-1800 nm (py) 1600±100 nm (py) 600-900 nm (p) sub-900 nm (p)	400 kHz (p) 100 kHz (p) 100 kHz (py) 1 kHz (c)				•	Gaikwad et al., 2020 [119]; Forien et al., 2020 [120]; Forien et al., 2023 [121]; Gorgannejad et al., 2023 [122]
University of Nebraska-Lincoln		•	•		950 nm (c) 700 nm (c) 700±5 nm (p) 650±5 nm (p) 350-1000 nm (p) visible-NIR (p)	100 kHz (c) 10 kHz (p)	•	•	•		Montazeri et al., 2018 [123]; Yavari et al., 2021 [124]; Gaikwad et al., 2022 [12]; King, 2022 [125]
Wuhan University		•			550 nm 630 nm 780 nm 905 nm	2 kHz 9 kHz	•	•	•		Li et al., 2025 [126]; Li et al., 2025 [127]; Lu et al., 2025 [128]
South China University of Technology		•	•		900 nm (c) 900±5 nm (p) 800±5 nm (p)	100 kHz (p) 5 kHz (c) 2 kHz (c)		•	•		Zhou et al., 2023 [129]; Zhou et al., 2023 [130]; Zhou et al., 2026 [131]
VTT Technical Research Centre of Finland; University of Turku			•		450-900 nm 400-800 nm 650±5 nm 636±5 nm	100 kHz					Reijonen et al., 2020 [132]; Reijonen et al., 2023 [133]; Reijonen et al., 2024 [134]
Luleå University of Technology				•	405, 450, 520, 580, 625, 850 nm 200-1100 nm	/					Brandau et al., 2022 [135]; Brandau et al., 2022 [136]; Brandau et al., 2024 [137]
Technical University of Darmstadt		•	•		950 nm (c) 900±50 nm (c) 400-900 nm (p)	60 kHz (p) 41.925 kHz (c) 41 kHz (c) 13.8 kHz (c)		•	•		Harbig et al., 2022 [138]; Merschroth et al., 2022 [139]; Weigold & Merschroth, 2023 [140]
Technical University of Denmark			•		1180-1800 nm 1100-1500 nm	100 kHz					Nadipalli et al., 2019 [141]; Andersen et al., 2022 [142]; Moshiri et al., 2023 [143]
Chalmers University of Technology		•	•		900±12.5 nm (c) 450-850 nm (p) visible and NIR (p)	60 kHz (p)					Schwerz & Nyborg, 2021 [144]; Schwerz, 2021 [145]; Schwerz, 2023 [146]
Chongqing Institute of Green and Intelligent Technology		•			sub-900 nm 400-530 nm	25 kHz 0.052-0.057 kHz		•	•		Zheng et al., 2019 [147]; Zhang et al., 2022 [148]; Zhang et al., 2023 [149]
University of Bordeaux			•		NIR	100 kHz					Yadav et al., 2021 [150]; Yadav et al., 2021 [151]; Yadav et al., 2022 [152]
Guangxi University		•			808 nm (illumination) (c) 780-1080 nm (IR c)	2 kHz (c) 0.06 kHz (IR c)		•	•		Wei et al., 2025 [153]; Zhang Yu. et al., 2025 [154]
Cyril and Methodius University in Skopje				•	400-900 nm (s)	/					Vasileska et al., 2024 [155]; Vasileska et al., 2025 [156]
Oak Ridge National Laboratory			•		NIR visible	60 kHz					Snow et al., 2023 [157]; Snow et al., 2023 [158]

Research group*	Used for control	Coaxial camera	Coaxial photodiode	Other coaxial sensors	Wavelengths c – camera p – photodiode py – pyrometer s – spectrometer o – other / - not specified or not found	Measuring frequency c – camera p – photodiode py – pyrometer s – spectrometer o – other / - not specified or not found	Two-color pyrometry	Temperature estimation	Meltpool depth estimation	Other meltpool dimensions est.	Publications
Purdue University		•	•		/	50 kHz (p) 30 kHz 15 kHz (c)				•	Raj et al., 2023 [159]; Raj et al., 2023 [160]
University of Sheffield	•	•		•	/	0.4 kHz (c)		•		•	Maddison, 2022 [161]; Lai et al., 2023 [162]
Beijing Institute of Technology		•	•		905±2 nm (c) 780±2 nm (c) 650-1000 nm (p)	3-10 kHz 0.3-8 kHz	•	•		•	Ma et al., 2022 [163]; Mao et al., 2023 [164]
Technical University of Munich		•	•		900±50 nm (c) 400–900 nm (p)	60 kHz (p) 20 kHz (c) 13.8 kHz (c)				•	Harbig et al., 2022 [138]; Grünewald et al., 2023 [165]
Seoul National University			•		NIR visible	60 kHz					Lee et al., 2022 [166]; Lee et al., 2023 [167]
Bremer Institut für angewandte Strahltechnik GmbH		•			667 nm 661 nm	0.2 kHz	•	•		•	Tyralla & Seefeld, 2021 [168]; Tyralla, & Seefeld, 2023 [169]
University of Massachusetts Amherst	•	•			850±20 nm	10 kHz 2 kHz				•	Yang et al., 2020 [26]; Fathizadan et al., 2023 [37]
Technische Hochschule Aschaffenburg			•		450-850 nm	60 kHz					Voigt et al., 2022 [170]; Voigt et al., 2022 [171]
Huazhong University of Science & Technology		•			/	10 kHz				•	Luo S. et al., 2021 [172]; Li et al., 2022 [173]
Huaqiao University					/	/					Xu et al., 2021 [174]; Xu et al., 2023 [175]
Fraunhofer Institute for Laser Technology ILT		•		•	2100 nm 1700 nm 1200-1900 nm (py) 1030 nm	100 kHz 0.3-100 kHz					Thombansen et al., 2015 [176]; Duong et al., 2022 [177]
Friedrich-Alexander-University		•	•		700-900 nm	40 kHz (p) 15 kHz (c)				•	Kolb et al., 2019 [178]; Kolb et al., 2020 [179]
University of Bremen	•			•	850-1000 nm	/					Renken et al., 2018 [180]; Renken et al., 2019 [181]
University of Duisburg-Essen; SLM Solutions			•		/	100 kHz					Alberts et al., 2016 [182]; Alberts et al., 2017 [183]
RWTH Aachen University; Federal Institute of Santa Catarina		•		•	1030 nm 1700 nm 2100 nm	0.3-100 kHz					Thombansen et al., 2014 [184]; Thombansen et al., 2015 [176]
École Nationale d'Ingénieurs de Saint-Etienne		•		•	900-1700 nm (py) 900 nm (c) 700 nm (c)	/	•	•			Chivel & Smurov, 2010 [185]; Smurov & Doubenskaia, 2012 [186]
Universität Innsbruck				•	1753 nm (py)	100 kHz			•	•	Stajkovic et al., 2025 [187]
amsight GmbH; Fraunhofer IAPT			•		visible IR	200 kHz 100 kHz					Lindecke et al., 2025 [188]
The University of Arizona		•			750-1000 nm	1 kHz					Hasan et al., 2025 [189]
Zhejiang Ocean University			•		800 nm	100 kHz					Zhou et al., 2026 [131]
Technical University of Madrid			•		700-1040 nm (p1), 1070-1700 nm (p2)	100 kHz					Wilkinson et al., 2025 [190]
Colorado School of Mines			•		785 nm	100 kHz					Hunter et al., 2025 [191]
Ghent University		•			850 nm	20 kHz					Booth et al., 2025 [192]
NASA Langley Research		•			725 nm 900 nm	2 kHz	•				Zalameda et al., 2025 [193]

Research group*	Used for control	Coaxial camera	Coaxial photodiode	Other coaxial sensors	Wavelengths c – camera p – photodiode py – pyrometer s – spectrometer o – other / - not specified or not found	Measuring frequency c – camera p – photodiode py – pyrometer s – spectrometer o – other / - not specified or not found	Two-color pyrometry	Temperature estimation	Meltpool depth estimation	Other meltpool dimensions est.	Publications
École Polytechnique Fédérale de Lausanne (EPFL) / Swiss Federal Institute of Technology Lausanne		•	•		IR 810-1000 nm 700-1000 nm 700-810 nm	0.15 kHz 50-100 kHz (p)	•	•		•	Esmaeilzadeh et al., 2025 [194]; Van Gestel, 2015 [230]
University of New South Wales			•		/	100 kHz					Liu, 2025 [195]
University College London			•		IR (p1) visible (p2)	/					Hocine et al., 2025 [196]
MIT - Massachusetts Institute of Technology					/	/					Penny et al., 2025 [197]
University of Michigan		•	•		700-1000 nm (c) 700-1000 nm (p)	2 kHz (c) 50 kHz (p)				•	Kirschbaum et al., 2025 [198]
National Yang Ming Chiao Tung University			•		350-1100 nm						Huang et al., 2024 [199]
Southeast University (China)			•		320-1000 nm	/					Zhou T. et al., 2024 [200]
Osaka University			•		NIR visible	60 kHz					Liu Y. et al., 2023 [201]
Drexel University			•		700±5 nm 650±5 nm	100-200 kHz	•	•			Tekerek et al., 2023 [202]
Fraunhofer Institute for High-Speed Dynamics				•	2000-2200 nm 1650-1800 nm 1580-2000 nm 1450-1700 nm	10 kHz	•	•			Pfaff et al., 2023 [203]
Bundesanstalt für Materialforschung und -prüfung (BAM)			•		/	/					Scheuschner et al., 2023 [204]
Arizona State University		•			NIR	10 kHz					Fathizadan et al., 2023 [37]
Flanders Make vzw		•			/	20 kHz					Blanc et al., 2023 [205]
Virginia Tech	•			•	/	2 kHz		•			Wang et al., 2023 [206]
University of Connecticut			•		1100–1700 nm 550–950 nm	100 kHz					Chen R. et al., 2023 [207]
Raytheon Technologies Research Center					/	/					Surana et al., 2023 [208]
GE Research; GE Additive		•	•		NIR (p) Visible (p)	60 kHz (p)					Felix et al., 2022 [209]
University of West Bohemia			•		400-900 nm	60 kHz					Bakir, 2022 [210]
Wuhan University of Science and Technology		•			850 nm	2 kHz				•	Lin et al., 2022 [211]
Kindai University		•			/	10 kHz	•	•		•	Ikeshoji et al., 2022 [212]
The University of Alabama in Huntsville			•		400-900 nm	16 kHz					Lanigan, 2022 [213]
Singapore University of Technology and Design				•	/	/					Balaraman et al., 2022 [214]
Pennsylvania State University			•		560±5 nm 580±5 nm	/					Przyjemski, 2021 [215]
The Ohio State University		•			IR	15 kHz				•	O'Loughlin et al., 2021 [216]
Robert Bosch GmbH		•			/	4 kHz					Slodczyk et al., 2021 [217]

Research group*	Used for control	Coaxial camera	Coaxial photodiode	Other coaxial sensors	Wavelengths c – camera p – photodiode py – pyrometer s – spectrometer o – other / - not specified or not found	Measuring frequency c – camera p – photodiode py – pyrometer s – spectrometer o – other / - not specified or not found	Two-color pyrometry	Temperature estimation	Meltpool depth estimation	Other meltpool dimensions est.	Publications
Technische Universität Dresden; Fraunhofer Institute for Machine Tools and Forming Technology (IWU)		•	•		/	40 kHz (p) 15 kHz (c)					Klein et al., 2021 [218]
University of Nottingham		•			950 nm 700 nm	100 kHz	•	•		•	Remani et al., 2021 [219]
Tusas Engine Industries Inc.			•		NIR	60 kHz					Dursun et al., 2020 [220]
Hamburg University of Technology			•		350-1100 nm	50 kHz					Fernandez et al., 2020 [221]
German Aerospace Center			•		/	50-100 kHz					Artzt et al., 2020 [222]
Technical University Berlin			•		/	/					Mohr et al., 2020 [223]
Ansys; Sigma Labs			•		/	200 kHz	•	•			Francis et al., 2019 [224]
Carnegie Mellon University		•			850±20 nm	50 kHz		•		•	Fisher, 2018 [225]; Fisher et al., 2018 [10]
Changchun University of Science and Technology		•			/	/		•			Liu C. et al., 2017 [226]
Queen's University		•		•	864 nm 843 nm	200 kHz					Kanko et al., 2016 [227]
EWI			•	•	350-1100 nm (p) 200-1100 nm (s)	1 kHz (s)					Jamshidinia et al., 2016 [228]
MerPhotonics		•			900-1200 nm (py) 850 nm (c)	20 kHz (p)	•	•			Chivel, 2016 [229]
Institute of Applied Physical Problems; École Nationale d'Ingénieurs de Saint-Etienne		•		•	900-1700 nm (py) 900 nm (c) 700 nm (c)	/	•	•			Chivel & Smurov, 2010 [185]

* The research group/institution listed in the first column corresponds to the affiliation of the first author of each publication or to an institution where the main experimental equipment is located (if the location of the equipment is possible to be recognized from the given information). Many of the listed publications involve collaborations with researchers from more than just one institution.

of references. Later in this document, the most important ones are highlighted and discussed.

3 COAXIAL MONITORING OF MELTPOOL DEPTH

The pressing problem in terms of control is that most existing coaxial measurement-based monitoring systems do not measure suitable variables for PBF-LB/M process control, at least not for all common scanning situations. For example, most of the existing systems measure the peak, average, or cumulative intensity of the emitted light, meltpool area, or meltpool temperature. The problem with these metrics is that they do not sufficiently describe process conditions to be able to make 'optimal' corrective control actions. For example, it has been shown that it is possible for deeper meltpools to have a smaller width than shallower meltpools (Rombouts et al. [231]; Bidare [232]; Andreau et al. [233]). This means that in some cases, for example, a possible lower cumulative intensity of the emitted light from the meltpool area may mean a deeper meltpool and keyhole, which is counterintuitive and requires opposite control logic compared to other typical process regimes.

Another potentially problematic situation for the interpretation of cumulative coaxial emission intensity occurs at sharp scan-direction changes, such as 180° turnarounds. During a straight scan segment, the meltpool and its elongated thermal tail have a relatively stable orientation with respect to the scan direction and the coaxial sensor field of view. At a sharp turnaround, however, the scan velocity and direction change rapidly, altering the geometry and orientation of the emitting meltpool region relative to the measurement field. Consequently, a different fraction of the meltpool and its surrounding heated region may contribute to the spatially integrated signal. For example, part of the meltpool tail may lie outside the effective measurement field during straight scanning but contribute differently to the measured signal during a turnaround. Thus, variations in

cumulative emission intensity at such locations cannot necessarily be attributed uniquely to changes in meltpool depth or energy input. This geometric ambiguity may limit the use of cumulative intensity alone as a feedback variable during highly transient scan trajectories and warrants dedicated experimental investigation.

A particularly important variable for controlling the PBF-LB/M process is meltpool depth, although depth should not necessarily be regarded as a complete standalone descriptor of the meltpool state. Meltpool depth provides information on penetration below the build surface that cannot be directly inferred from the apparent meltpool width, area, or cumulative optical emission. This distinction is important because insufficient penetration can contribute to lack-of-fusion, whereas excessive penetration associated with the formation of a deep and unstable keyhole can promote keyhole-induced porosity. At the same time, the studies of Rombouts et al. [231], Bidare [232], and Andreau et al. [233] indicate that meltpool dimensions can vary non-monotonically with one another; in particular, a deeper meltpool can under certain processing conditions be narrower than a shallower meltpool. Therefore, depth alone does not fully characterize the meltpool geometry.

From a process-control perspective, a multidimensional description incorporating meltpool depth together with surface-accessible dimensions may ultimately provide a more complete representation of the process state. For example, meltpool cross-sectional area, a depth-to-width ratio, or a three-dimensional/volumetric descriptor could potentially distinguish process states having similar depths but substantially different meltpool geometries. However, obtaining such descriptors in situ is considerably more challenging because the subsurface portion of the meltpool is not directly observable using conventional coaxial optical monitoring. Consequently, reliable high-resolution estimation of meltpool depth can be regarded as an important step toward more comprehensive meltpool-state estimation and control, rather than as a universally sufficient control variable by itself.

With the ability to control the meltpool depth, it is possible to avoid lack-of-fusion that would arise due to too shallow meltpool in the conductive welding mode on one side and keyhole pores due to too large and unstable keyhole in the keyhole regime on the other side. According to NASA Marshall Space Flight Center Specification MSFC-SPEC-3717, meltpool geometry, including meltpool depth, is an important indicator of process stability and consistency in laser powder bed fusion. Predicting meltpool depth can therefore provide a useful surrogate metric for assessing process conditions, with the potential to reduce the need for extensive post-process characterization. It also enables a quick check of how the microstructure is changing. The issue is that meltpool depth is not directly observable with the coaxial measurement system during the process. However, there have been some attempts to estimate the meltpool depth using coaxial measurement systems. Goossens and Van Hooreweder [70] at KU Leuven indirectly measured meltpool depth using coaxial camera measurements and a physics-based analytical model. There was an average error of 2.8 % to 9.9 % in the predicted meltpool depth. However, the system was not tested for all possible PBF-LB/M situations, such as 180° scan turnarounds or scanning above the overhang regions. Furthermore, it was tested only for SS316L printing material.

At the Polytechnic University of Milan, Caprio et al. [54] used a coaxial high-speed camera to observe oscillations of the meltpool surface. They showed that meltpool surface oscillation frequency is correlated with the meltpool depth. This approach leaves an unanswered question of whether such indirect meltpool depth measurements can detect rapid changes in the process conditions, which is a crucial requirement for fast dynamic control. The developed system was tested only for SS316L printing material.

At the University of Pittsburgh, Vallabh et al. [77] developed a method of predicting meltpool depth and grain length based on measurements from their camera-based two-wavelength imaging pyrometry system. They compared predicted meltpool depths with measurements from ex-situ microscopy. The depth-prediction experiments were single scan tracks on a bare IN718 substrate with no powder. Their results show that meltpool temperature derived from two-wavelength imaging pyrometry measurements is an important variable that helps to estimate the meltpool depth. They tested the developed system on IN718 printing material. Stajkovic et al. [187] used a coaxial pyrometer to estimate the meltpool depth on a powder-free tungsten substrate. The pyrometer measured emissions from the meltpool with a frequency of 100 kHz. To achieve different meltpool conditions, they varied primary PBF-LB/M process parameters.

The research team from Northwestern University in the U.S. demonstrated that the two-color pyrometry principle shows promising results in the prediction of the meltpool depth with the photodiode-based coaxial measuring system [3,61,63]. It was demonstrated that the concept of two-color pyrometry and a photodiode-based coaxial measurement system can estimate relative changes in the meltpool depth. However, they also observed several problems and limitations with this approach: (1) only relative changes in the meltpool depth can be measured, not absolute values; (2) relative changes in the meltpool depth can be estimated only for a limited range of process conditions, i.e., results indicate that changes in the meltpool depth can be estimated only for conduction welding mode and, also, it is not yet known if such a measuring approach for laser beam shapes other than Gaussian; (3) high-frequency variations in the coaxial photodiodes' signals are not related to actual variations in the meltpool depth, making direct closed-loop control of the meltpool depth difficult or impossible; (4) relative changes in the meltpool depth can be measured only when the laser power is kept constant; and (5) results indicated that shield gas flow might have an effect on coaxial measurements. The developed system was tested solely with AlSi10Mg printing material. The limitations of two-color pyrometry photodiode-based systems were also demonstrated by others. For example, Thombansen et al. [176] have demonstrated how in coaxial PBF-LB/M measuring systems rays with different wavelengths will fall on different positions of the sensor's detection surface. Galvoscanners in PBF-LB/M systems are optimized for the working laser wavelength, but all wavelengths that could be used to make coaxial measurements are different from the wavelength of the working laser beam. The relative orientation and position of the meltpool on the sensor's detection surface will differ depending on the target position on the powder bed, scanning speed, laser power, and laser spot moving direction. In summary, the existing research and practice [3,61,63,176,234] show that a relatively simple photodiode-based coaxial measuring system is not a suitable way to obtain reliable coaxial measurements of the meltpool depth for control purposes.

Table 2 provides a synthesized comparison of the five identified approaches, highlighting the sensing principle, investigated material, type of meltpool depth information obtained, reported validation or supporting evidence, and the principal limitations relevant to high-resolution process monitoring and control. The approaches differ in both measurement principle and maturity: they range from physics-based estimation using coaxial imaging and correlations with meltpool surface oscillations to two-wavelength imaging pyrometry, single-channel pyrometry, and two-color photodiode measurements.

The limitations identified for two-color photodiode-based depth estimation do not necessarily imply that the two-color measurement

Table 2. Comparison of reported approaches for coaxial estimation of meltpool depth in PBF-LB/M

Study	Coaxial sensing approach	Material	Meltpool-depth information	Validation / supporting evidence	Main limitations relevant to process monitoring and control
Goossens and Van Hooreweder [70]	Coaxial camera measurements combined with a physics-based analytical model	316L stainless steel	Absolute meltpool-depth prediction	Reported average prediction error of 2.8 % to 9.9 %	Evaluated only for 316L SS; not tested for all relevant PBF-LB/M scanning situations, including 180° scan turnarounds and scanning above overhang regions.
Caprio et al. [54]	Coaxial high-speed camera; analysis of meltpool-surface oscillations	316L stainless steel	Meltpool depth inferred from meltpool-surface oscillation frequency	Demonstrated correlation between meltpool-surface oscillation frequency and meltpool depth	Evaluated only for 316L SS; capability to detect sufficiently rapid changes in meltpool depth for fast dynamic process control remains an open question
Vallabh et al. [77]	Coaxial camera-based two-wavelength imaging pyrometry	IN718, powder-free substrate	Meltpool-depth prediction based on measured meltpool characteristics, including temperature	Predicted meltpool depths compared with measurements obtained from ex-situ microscopy; results indicate that temperature derived from two-wavelength imaging pyrometry provides useful information for depth estimation	Evaluated for IN718; validation across other materials and a broader range of processing conditions was not reported in the reviewed study
Stajkovic et al. [187]	Coaxial pyrometer; 100 kHz acquisition	Tungsten, powder-free substrate	Correlation/inference of melt-pool/keyhole depth from pyrometric signal and dimensionless-enthalpy model	Different meltpool conditions were generated by varying primary process parameters	Experiments were conducted on a powder-free tungsten substrate; applicability and transferability to powder-bed PBF-LB/M conditions require further validation
Kozjek et al. / Carter et al. [3,61,63]	Two-color coaxial photodiode measurements	AlSi10Mg	Relative changes in meltpool depth; absolute depth not obtained	Demonstrated that two-color pyrometry signals can provide information on relative changes in meltpool depth within a limited range of process conditions	Limited to relative depth changes and a restricted range of process conditions; demonstrated for conduction welding mode; constant laser power required; high-frequency photodiode-signal variations do not correspond to actual depth variations; applicability to non-Gaussian laser-beam shapes remains unknown; shield-gas flow may affect measurements; evaluated only for AlSi10Mg

principle itself is unsuitable for this purpose. Rather, some of the identified limitations may be associated with the spatially integrated nature of photodiode measurements. In this context, camera-based sensing provides an additional advantage by retaining spatially resolved, two-dimensional information about the meltpool and its surroundings. Combining this spatial information with measurements at two wavelength bands therefore represents a potentially promising direction for future meltpool-depth estimation. It should be emphasized, however, that most of the two-color camera-based systems that will be discussed below have not been developed or validated for meltpool-depth measurement. They are presented here as examples demonstrating the feasibility of spatially resolved two-wavelength meltpool monitoring and the extraction of meltpool characteristics, such as temperature and morphology, which could potentially provide inputs for future depth-estimation approaches. Figure 3 shows an example of a two-color camera-based coaxial meltpool monitoring system used by Hooper [94]. Figure 4 shows an example of meltpool temperature estimations obtained through that same system implemented by Hooper [94]. Additionally and equally important is the comprehensive evaluation of such measurement systems across all common PBF-LB/M processing conditions and widely used materials, including SS316L, IN718, Ti6Al4V, and AlSi10Mg. Besides the ability to avoid positional dependence issues common for other single-element (point) sensors, camera-based monitoring systems provide a more detailed view (2D image) of the main processing zone, i.e., the meltpool and its surroundings.

Several two-wavelength camera-based coaxial monitoring systems have already demonstrated these enabling capabilities. Chivel and Smurov [185] presented an early implementation in which meltpool radiation at 700 nm and 900 nm was imaged onto different regions of a camera sensor. Hooper [94] employed two coaxial cameras operating at 700 nm and 950 nm, respectively, to obtain spatially resolved two-color measurements of the meltpool. Ma et al. [163] used coaxial imaging at (780 ± 2) nm and (905 ± 2) nm to estimate meltpool surface-temperature distributions and cooling rates under different processing conditions. These studies did not demonstrate meltpool-depth estimation and are included here to illustrate existing implementations of spatially resolved two-wavelength coaxial sensing. In contrast, Vallabh et al. [77] used two-wavelength imaging pyrometry to predict meltpool depth, with the predicted values compared against ex-situ microscopy measurements.

Although this review focuses on the in-situ measuring method to estimate meltpool depth in PBF-LB/M, it is important to note that meltpool depth is not the only useful variable that is beneficial to improving control of the PBF-LB/M process. For example, in situ measuring techniques for measuring variables that are related to

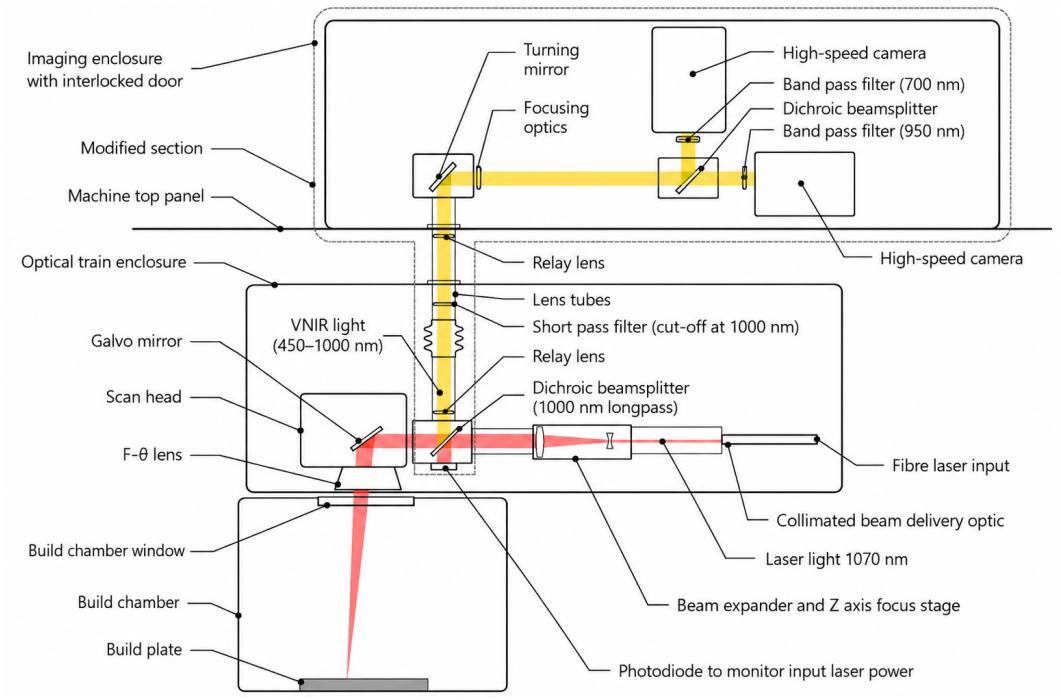


Fig. 3. Example of a two-color camera-based coaxial meltpool monitoring system demonstrating a measurement architecture potentially applicable to future meltpool-depth estimation. Source: Hooper [94]

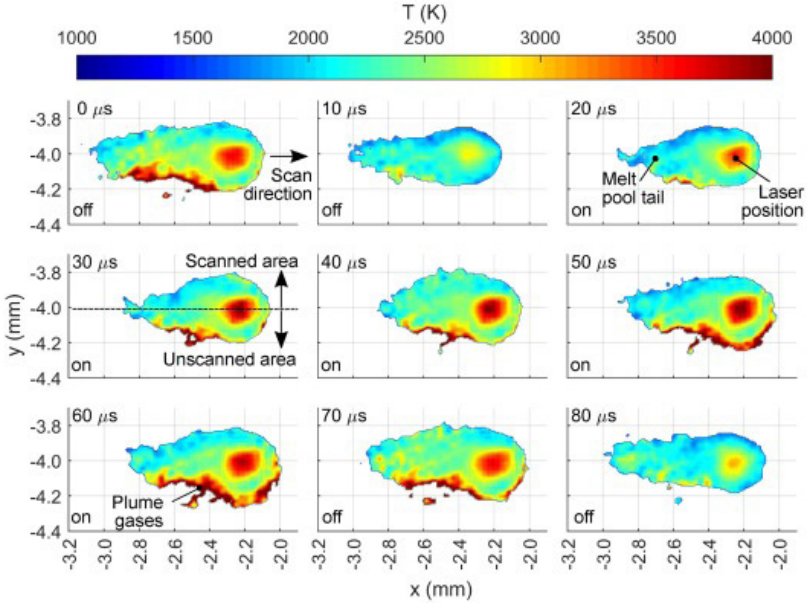


Fig. 4. Example of spatially resolved meltpool-temperature estimation obtained using the two-color camera-based coaxial monitoring system (does not represent meltpool-depth measurement). Source: Hooper [94]

residual stress would also improve the control [235], and they might also be possible via coaxial monitoring of the meltpool; however, until now, no evidence has been provided in the literature that this would be possible. Research in the field of coaxial monitoring of the meltpool is still in the stage where mainly direct variables, such as meltpool size and surface temperature, are estimated in situ. Coaxial monitoring is also promising to establish in situ defect detection systems, such as real-time photodiode-based keyhole-induced porosity detection systems [61,65], and outputs of such signals can also be considered in online control during the PBF-LB/M process.

4 WHAT TO CONSIDER IN IMPLEMENTATION OF COAXIAL MONITORING OF MELTPOOL IN PBF-LB/M

If one were to implement coaxial monitoring in an existing PBF-LB/M machine, there are several important things that must be considered:

- **Spectrum of the observed light:** Different materials have different emission spectra and discovered light emission phenomena from one material are not directly transferable to other materials. Currently, there are still many research gaps in terms of different materials and coaxial monitoring. For example, the list below summarizes the wavelength–material combinations

investigated by individual research groups in the field of camera-based coaxial two-color monitoring during PBF-LB/M; the corresponding publications and references are provided in Table 1:

- University of Pittsburgh, [550 nm, 620 nm], IN718
- Imperial College London, [700 nm, 950 nm], Ti6Al4V, SS316L
- University of Nebraska-Lincoln, [700 nm, 950 nm], IN718, SS316L
- Imperial College London, University of Nebraska-Lincoln, [700 nm, 950 nm], SS316L
- Wuhan University, [550 nm, 630 nm], IN718
- Beijing Institute of Technology, [780 nm, 905 nm], SS316L
- Bremer Institut für angewandte Strahltechnik GmbH, [661 nm, 667 nm], SS316L
- University of Nottingham, [700 nm, 950 nm], IN718
- Swiss Federal Institute of Technology Lausanne, [700 nm to 810 nm, 810-1000 nm], Maraging 300 steel, Ti6Al4V
- Institute of Applied Physical Problems, [700 nm, 900 nm], Inox 316
- NASA Langley Research, [725 nm, 900 nm], Ti6Al4V

In the list above, it can be observed that in most cases each group studied only one material on their two-color camera-based coaxial monitoring system. Below is also a list that shows what combinations of wavelength bands have been studied for individual printing material across all above-mentioned studies:

- IN718: [550 nm, 630 nm], [550 nm, 620 nm], [750 nm, 900 nm], [700 nm, 950 nm]
- Ti6Al4V: [725 nm, 900 nm], [700 nm, 950 nm]
- SS316L: [661 nm, 667 nm], [700 nm, 900 nm], [780 nm, 905 nm], [700 nm, 950 nm]
- Marag. 300 steel: [700 nm to 810 nm, 810 nm to 1000 nm]

The selection of the combination of the wavelength bands depends on the purpose of the monitoring system. For example, if the purpose is to estimate meltpool temperature based on the principle of two-color pyrometry, then the selected wavelength bands should not be too far from each other to make assumption of the same emissivity valid, but on the other side, the selected wavelength bands should not be too close to avoid high effect of the measurement noise. Plasma shielding is another phenomenon that must be taken into consideration when selecting the observed light wavelength bands. The three short tips when selecting observed light wavelength bands would be: 1) Check the spectrum of emitted light from the meltpool and transmitted through the optical system; 2) Avoid peaks in the spectra above black body radiation; 3) Check sensor responsivity curves – where sensors are most responsive/sensitive.

- **Transmitted light spectrum through the machine optics**: Machine optics are optimized for a working laser wavelength and it can block some parts of the spectrum for coaxial monitoring. For example, Hooper [94] performed a wavelength transmissivity test on the two-color camera-based coaxial monitoring system. The test using a spectrometer showed that wavelengths between 750 and 875 nm are almost completely blocked. The blockade is found to be due to the optical coating used on the galvanometer scanning mirrors. The spectrometer test served as the basis for further selection of the two wavelength bands for the camera-based monitoring system.
- **Attenuation**: Due to the transmissivity/reflectivity of the optical elements on the optical path for coaxial monitoring, such as lenses, mirrors, and filters, the light with a target wavelength coming from the meltpool can be significantly attenuated.
- **Spectral sensitivity of the camera/light sensor**: Each camera or light detection sensor has limited spectrum of responsivity. For example, typical CMOS camera spectral responsivity covers the 350 nm to 1050 nm range (UV to NIR). Also, spectral responsivity curve is not a flat-top function but it gets significantly weaker towards the edges of the responsivity spectrum.
- **Problem of difference between monitored light wavelength band and working laser wavelength**: Optics system of the PBF-LB/M system is developed/optimized for the working laser wavelength. The light from the meltpool that is measured by the coaxial monitoring system is significantly different from the working laser wavelength. As a result, the refraction angles of the observed light are different from the laser refraction angles.
- **Image/observation point focus**: A camera sensor or other type of light detector must be, in most cases, placed in the focus of the observed light emissions, which might not be a trivial task. Focal distance is a function of wavelength. For example, focal distances for the visible spectrum can be significantly different than focal distances for wavelengths in the NIR part of the spectrum. Focal distance can also be a function of the laser beam position in the printing plane.
- **Positional dependence of the intensity of transmitted light emissions**: Because PBF-LB/M machine optics are not made for wavelengths of observed light emissions from the meltpool, the angles of incidence of the observed light will vary with the different laser beam position in the scanning plane. Because optical elements such as mirrors and bandpass filters are used in the coaxial monitoring system, different incidence angles at the individual optical elements will result in different amounts of transmitted/reflected light through the optical system. It is possible to perform calibration for this; however, a performed calibration is valid only for exact specific positions and orientations of the optical system and its elements inside it. Slight changes in position or orientation of the optical system or individual optical elements will in most cases require new calibration.
- **Intensity resolution and digitization bit depth of the light sensor:** The required intensity resolution depends on the magnitude of the signal variations that need to be distinguished. For camera-based measurements, digitization bit depth provides one relevant specification: an 8-bit acquisition provides (2^8=256) discrete digital levels, whereas 12-bit and 16-bit acquisition provide 4,096 and 65,536 levels, respectively. Higher bit depth can therefore be beneficial when small spatial or temporal variations in meltpool emission occupy only a limited portion of the available measurement range. However, nominal bit depth should not be interpreted directly as effective intensity resolution. The practically usable resolution also depends on sensor noise, full-well capacity, exposure time, optical throughput, and how effectively the available dynamic range is utilized. Sensor selection and exposure should therefore be chosen such that the process-relevant intensity variations are sufficiently larger than the measurement noise while avoiding saturation of the brightest meltpool regions.
- **Spatial resolution of the camera:** Spatial resolution should be specified at the build plane (e.g., in µm/pixel) and selected according to the characteristic size of the meltpool feature that needs to be resolved. PBF-LB/M meltpools are typically on the order of tens to hundreds of micrometers in size [10]. For illustration, a spatial sampling of 1 µm/pixel represents a 200 µm characteristic meltpool dimension with approximately 200 pixels, whereas at 10 µm/pixel the same dimension is represented by approximately 20 pixels. Both can provide spatial information on meltpool geometry, although substantially different levels of detail are retained. At 200 µm/pixel, however, a 200 µm characteristic dimension corresponds to only approximately one pixel; consequently, meltpool shape, boundaries, and internal intensity or temperature gradients cannot be meaningfully resolved. Thus, "sufficient" spatial resolution should be defined relative to the smallest process feature that must be quantified rather than by a universal µm/pixel threshold. In practice, increasing spatial resolution may require reducing the field of view and/or the sensor region of interest and can reduce the maximum achievable acquisition frequency. The spatial and temporal resolution should

therefore be selected jointly according to the intended monitoring or control task.

- **Real-time feedback from the scanning head:** In many cases, it is necessary to know when in terms of current XY position on the scanning plane of the laser beam or in terms of position along the scan path an individual measurement was taken. In such cases, positional or temporal synchronization of the coaxial sensor and laser positioning system is required. This can be achieved, for example, by intercepting control signals for motors which move galvoscanner mirrors. Another challenge here is to achieve exact temporal synchronization when aligning galvoscanner command signals with the moments of capturing the coaxial measurements, especially when establishing/researching high resolution dynamic control approaches where, for example, laser power must be adjusted every few micrometers along the scanning path.
- **High frequency measurements:** To be able to observe fast dynamics of the observed meltpool area during the PBF-LB/M process, often a high frequency measurement system is required, even up to more than 100 kHz. This poses two challenges:
  - The need for high-speed measurement processing, especially in camera-based coaxial monitoring systems (for example, extracting the meltpool region and/or performing other transformations of the image to get the right information for control or just simply save the measurement timely is not a trivial task).
  - High volumes of measurement data to be saved (for example, 100 kHz measurements of process conditions during a typical PBF-LB/M job with only one photodiode with laser and galvoscanner mirror positions information can take several tens of GB).

  There exist computing devices called FPGAs (Field-Programmable Gate Arrays), which can help with the above-mentioned challenges. Such computing devices have already been used to make fast processing of measurements/information possible for the needs of PBF-LB/M process monitoring and control, for example, see [9,22,43,118,176,178,180–182,218,236].
- **Contamination of the optical system interior:** Inserting a beam splitter onto the optical axis requires (at least briefly) opening the optical system. This must be done with extreme care to avoid contamination of the interior of the optical system with dust particles or moisture.
- **Modifying optical system should be performed carefully:** PBF-LB/M machines usually do not include a beam splitter on the optical axis which is needed to enable coaxial monitoring. A beam splitter is typically inserted between the scanning head and the laser beam expander/collimator unit. When inserting the beam splitter, one should be extremely careful that 1) the laser beam, which continues to the scan head, is not moved laterally or angled, and 2) that the dust (particles in the air) does not come inside the optical system during the beam splitter insertion.
- **Support from the machine producer:** Especially if a PBF-LB/M machine is still in the warranty period, the insertion or any kind of other machine modification or intervention must be performed with the knowledge of and/or in cooperation with the machine manufacturer.

The above-described guidelines and challenges are based on the existing literature and hands-on experiences with establishing and working with coaxial monitoring systems.

5 CONCLUSIONS

Developing effective coaxial monitoring systems that would be directly useful for control of the PBF-LB/M process is still in the active research phase. Currently, no general and feasible solution exists to measure variables that would be directly usable for PBF-LB/M process control purposes. This paper reviews existing literature on coaxial monitoring systems for the PBF-LB/M. The main characteristics of the individual groups' coaxial monitoring systems are summarized. This systematically organized list can serve to identify research gaps or as a guide to find the group with the coaxial monitoring system with desired characteristics, e.g., to establish experimental collaboration or to find relevant datasets of the coaxial monitoring system studies. Based on all found literature, future development directions of effective coaxial monitoring systems for control in PBF-LB/M are proposed. The camera-based two-color coaxial monitoring approach seems to be the most promising research and development direction. Also, the list and examples of important things to be considered in the implementation of coaxial monitoring systems are provided and discussed.

References

[1] Gutknecht, K., Cloots, M., Wegener, K. Relevance of single channel signals for two-colour pyrometer process monitoring of laser powder bed fusion. *Int J Mechatron Manuf Syst 14* 111-127 (2021) **DOI:10.1504/IJMMS.2021.119152**.

[2] Yeung, H., Lane, B., Fox, J. Part geometry and conduction-based laser power control for powder bed fusion additive manufacturing. *Addit Manuf 30* 100844 (2019) **DOI:10.1016/j.addma.2019.100844**.

[3] Kozjek, D., Porter, C., Carter III, F.M., Mogonye, J.-E., Cao, J. Data-driven prediction of geometry- and toolpath sequence-dependent intra-layer process conditions variations in laser powder bed fusion. *J Manuf Process 100* 34-46 (2023) **DOI:10.1016/j.jmapro.2023.05.021**.

[4] Yeung, H., Lane, B. A residual heat compensation based scan strategy for powder bed fusion additive manufacturing. *Manuf Lett 25* 56-59 (2020) **DOI:10.1016/j.mfglet.2020.07.005**.

[5] Carter III, F.M., Porter, C., Kozjek, D., Shimoyoshi, K., Fujishima, M., Irino, N. et al. Machine learning guided adaptive laser power control in selective laser melting for pore reduction. *CIRP Ann 73* 149-152 (2024) **DOI:10.1016/j.cirp.2024.04.043**.

[6] Wang, Q., Michaleris, P.P., Nassar, A.R., Irwin, J.E., Ren, Y., Stutzman, C.B. Model-based feedforward control of laser powder bed fusion additive manufacturing. *Addit Manuf 31* 100985 (2020) **DOI:10.1016/j.addma.2019.100985**.

[7] Taylor, H.C., Wicker, R.B. Impacts of microsecond control in laser powder bed fusion processing. *Addit Manuf 60* 103239 (2022) **DOI:10.1016/j.addma.2022.103239**.

[8] Reiff, C., Bubeck, W., Krawczyk, D., Steeb, M., Lechler, A., Verl, A. Learning feedforward control for laser powder bed fusion. *Procedia CIRP 96* 127-132 (2021) **DOI:10.1016/j.procir.2021.01.064**.

[9] Yeung, H. Toward Real-time feedback control for powder bed fusion additive manufacturing. *Addit Manuf 114* 105041 (2025) **DOI:10.1016/j.addma.2025.105041**.

[10] Fisher, B.A., Lane, B., Yeung, H., Beuth, J. Toward determining melt pool quality metrics via coaxial monitoring in laser powder bed fusion. *Manuf Lett 15* 119-121 (2018) **DOI:10.1016/j.mfglet.2018.02.009**.

[11] Zhang, Y., Hong, G.S., Ye, D., Zhu, K., Fuh, J.Y.H. Extraction and evaluation of melt pool, plume and spatter information for powder-bed fusion AM process monitoring. *Mater Des 156* 458-469 (2018) **DOI:10.1016/j.matdes.2018.07.002**.

[12] Gaikwad, A., Williams, R.J., de Winton, H., Bevans, B.D., Smoqi, Z., Rao, P., et al. Multi phenomena melt pool sensor data fusion for enhanced process monitoring of laser powder bed fusion additive manufacturing. *Mater Des 221* 110919 (2022) **DOI:10.1016/j.matdes.2022.110919**.

[13] Everton, S.K., Hirsch, M., Stravroulakis, P., Leach, R.K., Clare, A.T. Review of in-situ process monitoring and in-situ metrology for metal additive manufacturing. *Mater Des 95* 431-445 (2016) **DOI:10.1016/j.matdes.2016.01.099**.

[14] Pal, S., Finšgar, M., Vajda, J., Maver, U., Brajlih, T., Gubeljak, N., et al. Fusion behavior of pure magnesium during selective laser melting. *Stroj Vestn-J Mech Eng 71* 318-327 (2025) **DOI:10.5545/sv-jme.2025.1381**.

[15] Grasso, M., Colosimo, B.M. Process defects and in situ monitoring methods in metal powder bed fusion: a review. *Meas Sci Technol 28* 044005 (2017) **DOI:10.1088/1361-6501/aa5c4f**.

[16] McCann, R., Obeidi, M.A., Hughes, C., McCarthy, É., Egan, D.S., Vijayaraghavan, R.K. et al. In-situ sensing process monitoring and machine control in Laser Powder Bed Fusion: A review. *Addit Manuf 45* 102058 (2021) **DOI:10.1016/j.addma.2021.102058**.

[17] Grasso, M., Remani, A., Dickins, A., Colosimo, B.M., Leach, R.K. In-situ measurement and monitoring methods for metal powder bed fusion: an updated review. *Meas Sci Technol 32* 112001 (2021) **DOI:10.1088/1361-6501/ac0b6b**.

[18] Hou, Z.-J., Wang, Q., Zhao, C.-G., Zheng, J., Tian, J.-M., Ge, X.-H. et al. Online monitoring technology of metal powder bed fusion processes: A review. *Materials 15* 7598 (2022) **DOI:10.3390/ma15217598**.

[19] Cai, Y., Xiong, J., Chen, H., Zhang, G. A review of in-situ monitoring and process control system in metal-based laser additive manufacturing. *J Manuf Syst 70* 309-326 (2023) **DOI:10.1016/j.jmsy.2023.07.018**.

[20] Chen, L., Bi, G., Yao, X., Su, J., Tan, C., Feng, W. et al. In-situ process monitoring and adaptive quality enhancement in laser additive manufacturing: a critical review. *J Manuf Syst 74* 527-574 (2024) **DOI:10.1016/j.jmsy.2024.04.013**.

[21] Papatheodorou, A., Papadimitriou, N., Stathatos, E., Benardos, P., Vosniakos, G.-C. Recent advances in sensor fusion monitoring and control strategies in laser powder bed fusion: A review. *Machines 13* 820 (2025) **DOI:10.3390/machines13090820**.

[22] Lane, B., Mekhontsev, S., Grantham, S., Vlasea, M.L., Whiting, J., Yeung, H., et al. Design, Developments, and Results from the NIST Additive Manufacturing Metrology Testbed (AMMT) (2016).

[23] Lane, B., Grantham, S., Yeung, H., Zarobila, C., Fox, J. Performance characterization of process monitoring sensors on the NIST Additive Manufacturing Metrology Testbed (2017).

[24] Fox, J.C., Lane, B.M., Yeung, H. Measurement of process dynamics through coaxially aligned high speed near-infrared imaging in laser powder bed fusion additive manufacturing. *Thermosense: Thermal Infrared Applications XXXIX, SPIE* 34-50 (2017) **DOI:10.1117/12.2263863**.

[25] Yeung, H., Lane, B.M., Donmez, M.A., Fox, J.C., Neira, J. Implementation of advanced laser control strategies for powder bed fusion systems. *Procedia Manuf 26* 871-879 (2018) **DOI:10.1016/j.promfg.2018.07.112**.

[26] Yang, Z., Lu, Y., Yeung, H., Krishnamurty, S. From scan strategy to melt pool prediction: A neighboring-effect modeling method. *J Comput Inf Sci Eng 20* 051001 (2020) **DOI:10.1115/1.4046335**.

[27] Lane, B., Zhirnov, I., Mekhontsev, S., Grantham, S., Ricker, R., Rauniyar, S., et al. Transient laser energy absorption, co-axial melt pool monitoring, and relationship to melt pool morphology. *Addit Manuf 36* 101504 (2020) **DOI:10.1016/j.addma.2020.101504**.

[28] Lane, B., Jacquemetton, L., Piltch, M., Beckett, D. *Thermal Calibration of Commercial Melt Pool Monitoring Sensors on a Laser Powder Bed Fusion System*. National Institute of Standards and Technology, US Department of Commerce. (2020) **DOI:10.6028/NIST.AMS.100-35**.

[29] Lane, B., Yeung, H. Process monitoring dataset from the additive manufacturing metrology testbed (AMMT): Overhang part x4. *J Res Natl Inst Stand Technol 125* 125027 (2020) **DOI:10.6028/jres.125.027**.

[30] Yeung, H., Yang, Z., Yan, L. A meltpool prediction based scan strategy for powder bed fusion additive manufacturing. *Addit Manuf 35* 101383 (2020) **DOI:10.1016/j.addma.2020.101383**.

[31] Feng, S.C., Lu, Y., Jones, A.T. Measured data alignments for monitoring metal additive manufacturing processes using laser powder bed fusion methods. *International Design Engineering Technical Conferences and Computers and Information in Engineering Conference* V009T09A022 (2020) **DOI:10.1115/DETC2020-22478**.

[32] Feng, S.C., Lu, Y., Jones, A.T. Meta-data for in-situ monitoring of laser powder bed fusion processes. *International Manufacturing Science and Engineering Conference* V001T01A026 (2020) **DOI:10.1115/1.0002365V**.

[33] Lu, Y., Yang, Z., Kim, J., Cho, H., Yeung, H. Camera-based coaxial melt pool monitoring data registration for laser powder bed fusion additive manufacturing. *ASME International Mechanical Engineering Congress and Exposition* V02BT02A045 (2020) **DOI:10.1115/IMECE2020-24546**.

[34] Yang, Z., Lu, Y., Lane, B., Kim, J., Ndiaye, Y., Krishnamurty, S. *Analyzing Remelting Conditions based on In-Situ Melt Pool Data Fusion for Overhang Building in Powder Bed Fusion Process* (2021).

[35] Kim, F.H., Yeung, H., Garboczi, E.J. Characterizing the effects of laser control in laser powder bed fusion on near-surface pore formation via combined analysis of in-situ melt pool monitoring and X-ray computed tomography. *Addit Manuf 48* 102372 (2021) **DOI:10.1016/j.addma.2021.102372**.

[36] Yang, Z., Lane, B., Lu, Y., Yeung, H., Kim, J., Ndiaye, Y., et al. Using coaxial melt pool monitoring images to estimate cooling rate for powder bed fusion additive manufacturing. *International Design Engineering Technical Conferences and Computers and Information in Engineering Conference* V002T02A016 (2022) **DOI:10.1115/DETC2022-89934**.

[37] Fathizadan, S., Ju, F., Lu, Y., Yang, Z. Deep spatio-temporal anomaly detection in laser powder bed fusion. *IEEE Trans Autom Sci Eng 21* 5227-5239 (2023) **DOI:10.1109/TASE.2023.3309927**.

[38] Liu, X., Liu, X., Kumar, N.G., Witherell, P. Scalable path level thermal history simulation of powder bed fusion process validated by melt pool images. *Addit Manuf 84* 104111 (2024) **DOI:10.1016/j.addma.2024.104111**.

[39] Chen, H., Liu, X., Liu, X., Witherell, P. MeltpoolGAN: Melt pool prediction from path-level thermal history. *Addit Manuf 84* 104095 (2024) **DOI:10.1016/j.addma.2024.104095**.

[40] Kim, J., Yang, Z., Lu, Y. A physics-guided deep generative model for predicting melt pool behavior in laser powder bed fusion additive manufacturing. *J Intell Manuf 36* 5715-5735 (2025) **DOI:10.1007/s10845-024-02504-1**.

[41] Hong, G., Kim, J., Yang, Z., Lu, Y., Lane, B., Yeung, H. Multi-scale model predictive control for laser powder bed fusion additive manufacturing. *International Design Engineering Technical Conferences and Computers and Information in Engineering Conference* V02BT02A018 (2024) **DOI:10.1115/DETC2024-143601**.

[42] Yang, Z., Kim, J., Lane, B., Lu, Y. Measuring overhang down-skin dross depth and the inter-dependency on melt pool for laser powder bed fusion additive manufacturing. *International Manufacturing Science and Engineering Conference* V001T01A020 (2024) **DOI:10.1115/MSEC2024-124322**.

[43] Yang, C.-W., Hong, G., Yang, Z., Philomin, S., Li, S., Lu, Y., et al. FPGA implementation for advanced real-time melt pool monitoring of laser powder bed fusion processes. *International Design Engineering Technical Conferences and Computers and Information in Engineering Conference* V02BT02A043 (2025) **DOI:10.1115/DETC2025-168460**.

[44] Hong, G.S., Yang, Z., Yang, C., Lu, Y., Cho, H. Track-wise melt pool prediction for laser powder bed fusion process control. *International Design Engineering Technical Conferences and Computers and Information in Engineering Conference* V02AT02A050 (2025) **DOI:10.1115/DETC2025-167958**.

[45] Bozzani, M., Beretta, D. *Coaxial Monitoring with Multiple Sensors and Defect Correction for Selective Laser Melting* (2015).

[46] Demir, A.G., De Giorgi, C., Previtali, B. Design and implementation of a multisensor coaxial monitoring system with correction strategies for selective laser melting of a maraging steel. *J Manuf Sci Eng 140* 041003 (2018) **DOI:10.1115/1.4038568**.

[47] Bejan, C.C. Development of a Coaxial Monitoring System for the Sensing of Melt Pool Surface Oscillations in the SLM Process (2018).

[48] Vasileska, E. *Improving Melt Pool Stability in Selective Laser Melting by Empirical Modelling and Layerwise Control of Temporal Emission Profile.* MSc Thesis, Politecnico Milano, Milano (2019) **https://hdl.handle.net/10589/147269**.

[49] Mazzoleni, L., Caprio, L., Pacher, M., Demir, A.G., Previtali, B. External Illumination strategies for melt pool geometry monitoring in SLM. *JOM 71* 928-937 (2019) **DOI:10.1007/s11837-018-3209-1**.

[50] Mazzoleni, L., Demir, A.G., Caprio, L., Pacher, M., Previtali, B. Real-time observation of melt pool in selective laser melting: spatial, temporal, and wavelength resolution criteria. *IEEE Trans Instrum Meas 69* 1179-1190 (2019) **DOI:10.1109/TIM.2019.2912236**.

[51] Pacher, M., Mazzoleni, L., Caprio, L., Demir, A.G., Previtali, B. Estimation of melt pool size by complementary use of external illumination and process emission in coaxial monitoring of selective laser melting. *J Laser Appl 31* (2019) **DOI:10.2351/1.5096117**.

[52] Demir, A.G., Mazzoleni, L., Caprio, L., Pacher, M., Previtali, B. Complementary use of pulsed and continuous wave emission modes to stabilize melt pool geometry in laser powder bed fusion. *Opt Laser Technol 113* 15-26 (2019) **DOI:10.1016/j.optlastec.2018.12.005**.

[53] Vasileska, E., Demir, A.G., Colosimo, B.M., Previtali, B. Layer-wise control of selective laser melting by means of inline melt pool area measurements. *J Laser Appl 32* (2020) **DOI:10.2351/7.0000108**.

[54] Caprio, L., Demir, A.G., Previtali, B. External illumination enables coaxial sensing of surface and subsurface molten pool geometry in LPBF. *Metals 12* 1762 (2022) **DOI:10.3390/met12101762**.

[55] Vasileska, E., Demir, A.G., Colosimo, B.M., Previtali, B. A novel paradigm for feedback control in LPBF: layer-wise correction for overhang structures. *Adv Manuf 10* 326-344 (2022) **DOI:10.1007/s40436-021-00379-6**.

[56] Gronle, M., Grasso, M., Granito, E., Schaal, F., Colosimo, B.M. Open data for open science in Industry 4.0: In-situ monitoring of quality in additive manufacturing. *J Qual Technol 55* 253-265 (2023) **DOI:10.1080/00224065.2022.2106910**.

[57] Cacace, S., Bugatti, M., Colosimo, B.M. From design to reality: Improving multimaterial powder bed fusion laser melting additive manufacturing via in-situ monitoring. *Italian Manufacturing Association Conference 216* (2025) **DOI:10.21741/9781644903735-25**.

[58] Kozjek, D., Carter III, F.M., Porter, C., Mogonye, J.-E., Ehmann, K., Cao, J. Data-driven prediction of next-layer melt pool temperatures in laser powder bed fusion based on co-axial high-resolution Planck thermometry measurements. *J Manuf Process 79* 81-90 (2022) **DOI:10.1016/j.jmapro.2022.04.033**.

[59] Porter, C., Carter, F., Kozjek, D., Cardona, A., Mogonye, J.-E., Ehmann, K., et al. *Generation and Analysis of AlSi10Mg L-PBF Single Track Data Set Enabling Deeper Process Insights* (2022) **DOI:10.26153/tsw/44250**.

[60] Kozjek, D., Porter, C., Carter III, F.M., Bhattad, P., Brackman, P., Lisovich, A. et al. Iterative closest point-based data fusion of non-synchronized in-situ and ex-situ data in laser powder bed fusion. *J Manuf Syst 66* 179-199 (2023) **DOI:10.1016/j.jmsy.2022.12.007**.

[61] Carter III, F.M., Kozjek, D., Porter, C., Clark, S.J., Fezzaa, K., Fujishima, M., et al. Melt pool instability detection using coaxial photodiode system validated by in-situ X-ray imaging. *CIRP Ann 72* 205-208 (2023) **DOI:10.1016/j.cirp.2023.03.031**.

[62] Liao, S., Xue, T., Cao, J. Deep learning based reconstruction of transient 3D melt pool geometries in laser powder bed fusion from coaxial melt pool images. *Manuf Lett 40* 50-53 (2024) **DOI:10.1016/j.mfglet.2024.02.005**.

[63] Kozjek, D., Porter, C., Carter, F.M., Mogonye, J.-E., Cao, J. Data-driven prediction of inter-layer process condition variations in laser powder bed fusion. *Addit Manuf 88* 104230 (2024) **DOI:10.1016/j.addma.2024.104230**.

[64] Samaei, A., Porter, C., Kozjek, D., Mogonye, J.-E., Cao, J., Wagner, G.J., Understanding coaxial photodiode-based multispectral pyrometer measurements at the overhang regions in laser powder bed fusion for part qualification. *Addit Manuf 93* 104398 (2024) **DOI:10.1016/j.addma.2024.104398**.

[65] Meng, C., Porter, C., Estalaki, S.M., Yang, S., Mathesen, G., Cao, J. Part-scale keyhole pore detection in laser powder bed fusion using coaxial photodiodes. *Addit Manuf 114* 105031 (2025) **DOI:10.1016/j.addma.2025.105031**.

[66] Kruth, J.-P., Mercelis, P., Van Vaerenbergh, J., Craeghs, T. Feedback control of selective laser melting. *Virtual and Rapid Manufacturing*, CRC Press 521-528 (2007).

[67] Berumen, S., Bechmann, F., Lindner, S., Kruth, J.-P., Craeghs, T. Quality control of laser-and powder bed-based additive manufacturing (AM) technologies. *Phys Procedia 5* 617-622 (2010) **DOI:10.1016/j.phpro.2010.08.089**.

[68] Craeghs, T., Bechmann, F., Berumen, S., Kruth, J.-P. Feedback control of layerwise laser melting using optical sensors. *Phys Procedia 5* 505-514 (2010) **DOI:10.1016/j.phpro.2010.08.078**.

[69] Clijsters, S., Craeghs, T., Buls, S., Kempen, K., Kruth, J.-P. In situ quality control of the selective laser melting process using a high-speed, real-time melt pool monitoring system. *Int J Adv Manuf Technol 75* 1089-1101 (2014) **DOI:10.1007/s00170-014-6214-8**.

[70] Goossens, L.R., Van Hooreweder, B. A virtual sensing approach for monitoring melt-pool dimensions using high speed coaxial imaging during laser powder bed fusion of metals. *Addit Manuf 40* 101923 (2021) **DOI:10.1016/j.addma.2021.101923**.

[71] Thanki, A., Goossens, L., Ompusunggu, A.P., Bayat, M., Bey-Temsamani, A., Van Hooreweder, B. et al. Melt pool feature analysis using a high-speed coaxial monitoring system for laser powder bed fusion of Ti-6Al-4V grade 23. *Int J Adv Manuf Technol 120* 6497-6514 (2022) **DOI:10.1007/s00170-022-09168-2**.

[72] Tao, Z., Thanki, A., Goossens, L., Witvrouw, A., Vrancken, B., Dewulf, W. Porosity prediction in selective laser melting combining photodiode-based in-process monitoring and X-CT. *e-J Nondestr Test* (2023).

[73] Thanki, A., Haitjema, H., Witvrouw, A. Correlation Between In-Process Melt Pool Monitoring and Post Process Characterization for Laser Powder Bed Fusion, (2024).

[74] Tao, Z., Thanki, A., Goossens, L., Witvrouw, A., Vrancken, B., Dewulf, W. Photodiode-based porosity prediction in laser powder bed fusion considering inter-hatch and inter-layer effects. *J Mater Process Technol 332* 118539 (2024) **DOI:10.1016/j.jmatprotec.2024.118539**.

[75] Vallabh, C.K.P., Zhao, X. Melt pool temperature measurement and monitoring during laser powder bed fusion based additive manufacturing via single-camera two-wavelength imaging pyrometry (STWIP). *J Manuf Process 79* 486-500 (2022) **DOI:10.1016/j.jmapro.2022.04.058**.

[76] Vallabh, C.K.P., Hinnebusch, S., To, A.C., Zhao, X. Layer-wise melt pool temperature evolution in laser powder bed fusion: An experimental study using a single camera based two-wavelength imaging pyrometry. *International Manufacturing Science and Engineering Conference* V002T05A032 (2022) **DOI:10.1115/MSEC2022-85387**.

[77] Vallabh, C.K.P., Sridar, S., Xiong, W., Zhao, X. Predicting melt pool depth and grain length using multiple signatures from in-situ single camera two-wavelength imaging pyrometry for laser powder bed fusion. *J Mater Process Technol 308* 117724 (2022) **DOI:10.1016/j.jmatprotec.2022.117724**.

[78] Zhang, H., Vallabh, C.K.P., Zhao, X. Registration and fusion of large-scale melt pool temperature and morphology monitoring data demonstrated for surface topography prediction in LPBF. *Addit Manuf 58* 103075 (2022) **DOI:10.1016/j.addma.2022.103075**.

[79] Vallabh, C.K.P., Zhao, X. Continuous comprehensive monitoring of melt pool morphology under realistic printing scenarios with laser powder bed fusion. *3D Print Addit Manuf 10* 101-110 (2023) **DOI:10.1089/3dp.2021.0060**.

[80] Zhao, X., To, A., Neu, R. *An Effective Quality Assurance Method for Additively Manufactured Gas Turbine Metallic Components via Machine Learning From In-Situ Monitoring, Part-Scale Modeling, and Ex-Situ Characterization Data*, University of Pittsburgh, Pittsburgh (2024).

[81] Akhavan, J., Vallabh, C.K., Zhao, X., Manoochehri, S. Binocular Model: A deep learning solution for online melt pool temperature analysis using dual-wavelength imaging pyrometry. *ArXiv Preprint* ArXiv:2408.11126 (2024).

[82] Alam, M.J., Zhang, H., Zhao, X. Enhancing image processing in single-camera two-wavelength imaging pyrometry for advanced in-situ melt pool measurement in laser powder bed fusion. *Precis Eng 93* 1-17 (2025) **DOI:10.1016/j.precisioneng.2024.12.013**.

[83] Zou, Z., Zhang, K., Liu, T., Li, J., Zhu, Z., Wei, H., et al. In situ monitoring with melt pool data based on multi-signal fusion method in laser powder bed fusion. *Measurement* 234 114877 (2024) **DOI:10.1016/j.measurement.2024.114877**.

[84] Li, J., Zhang, K., Liu, T., Wei, H., Chen, R., Guo, S., et al. Unsupervised learning-based identification of pore-prone regions via in-situ melt pool monitoring in thin-walled structures during laser powder bed fusion. *J Manuf Process 157* 1-14 (2026) **DOI:10.1016/j.jmapro.2025.11.069**.

[85] Li, J., Zhang, K., Liao, W., Liu, T., Zou, Z., Chen, R., et al. Evolution and prediction of lack of fusion pores in laser powder bed fusion process based on in-situ monitoring. *Measurement 245* 116617 (2025) **DOI:10.1016/j.measurement.2024.116617**.

[86] Li, J., Zhang, K., Liu, T., Zhu, Z., Zou, Z., Wei, H., et al. A novel extraction and evaluation method for melt pool images in laser powder bed fusion. *Opt Laser Technol 191* 113333 (2025) **DOI:10.1016/j.optlastec.2025.113333**.

[87] Zou, Z., Zhang, K., Liu, T., Wei, H., Chen, R., Liao, W. In-situ monitoring of porous struts via photodiode signals in laser powder bed fusion lattice structures. *J Manuf Process 156* 142-162 (2025) **DOI:10.1016/j.jmapro.2025.10.100**.

[88] Taherkhani, K., Sheydaeian, E., Eischer, C., Otto, M., Toyserkani, E. Development of a defect-detection platform using photodiode signals collected from the melt pool of laser powder-bed fusion. *Addit Manuf 46* 102152 (2021) **DOI:10.1016/j.addma.2021.102152**.

[89] Taherkhani, K., Eischer, C., Toyserkani, E. An unsupervised machine learning algorithm for in-situ defect-detection in laser powder-bed fusion. *J Manuf Process 81* 476-489 (2022) **DOI:10.1016/j.jmapro.2022.06.074**.

[90] Taherkhani, K. In-Situ Monitoring and Quality Assurance Algorithms for Laser Powder-Bed Fusion. PhD Thesis, University of Waterloo, Waterloo (2022) **Handle:10012/18142**.

[91] Taherkhani, K., Cantzler, G., Eischer, C., Toyserkani, E. Development of control systems for laser powder bed fusion. *Int J Adv Manuf Technol 129* 5493-5514 (2023) **DOI:10.1007/s00170-023-12663-9**.

[92] Liravi, F., Soo, S., Toorandaz, S., Taherkhani, K., Habibnejad-Korayem, M., Toyserkani, E. Tailoring laser powder bed fusion process parameters for standard and Off-size Ti6Al4V metal powders: A machine learning approach enhanced by photodiode-based melt pool monitoring. *Inventions 9* 87 (2024) **DOI:10.3390/inventions9040087**.

[93] Toorandaz, S., Taherkhani, K., Liravi, F., Toyserkani, E. A novel machine learning-based approach for in-situ surface roughness prediction in laser powder-bed fusion. *Addit Manuf 91* 104354 (2024) **DOI:10.1016/j.addma.2024.104354**.

[94] Hooper, P.A. Melt pool temperature and cooling rates in laser powder bed fusion. *Addit Manuf 22* 548-559 (2018) **DOI:10.1016/j.addma.2018.05.032**.

[95] de Winton, H.C., Cegla, F., Hooper, P.A. A method for objectively evaluating the defect detection performance of in-situ monitoring systems. *Addit Manuf 48* 102431 (2021) **DOI:10.1016/j.addma.2021.102431**.

[96] Larsen, S., Hooper, P.A. *Quantifying Defect Formation Signatures in Laser Powder Bed Fusion Through Melt Pool Imaging and Data-Driven Analysis*. Joint Special Interest Group Meeting between Euspen and ASPE Advancing Precision in Additive Manufacturing KU Leuven, (2023).

[97] Taylor, P.L., Williams, R.J., de Winton, H.C., Fernandez, V., Larsen, S., Hooper, P.A. Digital 3D defect maps: Detecting localised porosity with high-speed melt pool imaging data in LPBF. *Addit Manuf 111* 104982 (2025) **DOI:10.1016/j.addma.2025.104982**.

[98] Shkoruta, A., Caynoski, W., Mishra, S., Rock, S. Iterative learning control for power profile shaping in selective laser melting. *IEEE 15th International Conference on Automation Science and Engineering* 655-660 (2019) **DOI:10.1109/COASE.2019.8843070**.

[99] Shkoruta, A., Mishra, S., Rock, S. An experimental study on process modeling for selective laser melting. *IEEE American Control Conference* 467-473 (2020) **DOI:10.23919/ACC45564.2020.9147644**.

[100] Park, B., Wang, X., Mishra, S., Bristow, D., Landers, R. Melt pool feature extraction, spatial registration, and layer-to-layer control in powder bed fusion. *Proceedings of the 33rd Annual International Solid Freeform Fabrication Symposium* 1052-1061 (2022).

[101] Shkoruta, A., Mishra, S., Rock, S.J. Real-time image-based feedback control of laser powder bed fusion. *ASME Lett Dyn Sys Control 2* 021001 (2022) **DOI:10.1115/1.4051588**.

[102] Park, B., Chen, A., Mishra, S. Real-time melt pool homogenization through geometry-informed control in laser powder bed fusion using reinforcement learning. *IEEE Trans Autom Sci Eng 22* 2986-2997 (2024) *DOI:10.1109/TASE.2024.3386882*.

[103] Egan, D.S., Dowling, D.P. Influence of process parameters on the correlation between in-situ process monitoring data and the mechanical properties of Ti-6Al-4V non-stochastic cellular structures. *Addit Manuf 30* 100890 (2019) **DOI:10.1016/j.addma.2019.100890**.

[104] Egan, D.S., Jones, K., Dowling, D.P. Selective laser melting of Ti-6Al-4V: Comparing µCT with in-situ process monitoring data. *CIRP J Manuf Sci Technol 31* 91-98 (2020) **DOI:10.1016/j.cirpj.2020.10.004**.

[105] Egan, D.S., Dowling, D.P. Correlating in-situ process monitoring data with the reduction in load bearing capacity of selective laser melted Ti-6Al-4V porous biomaterials. *J Mech Behav Biomed Mater 106* 103723 (2020) **DOI:10.1016/j.jmbbm.2020.103723**.

[106] Keaveney, S., Shmeliov, A., Nicolosi, V., Dowling, D.P. Investigation of process by-products during the selective laser melting of Ti6AL4V powder. *Addit Manuf 36* 101514 (2020) **DOI:10.1016/j.addma.2020.101514**.

[107] Power, J.J., Humphreys, O., Hartnett, M., Egan, D., Dowling, D.P. Application of in situ process monitoring to optimise laser parameters during laser powder bed fusion printing of Ti-6Al-4V parts with overhang structures. *Int J Adv Manuf Technol 130* 2297-2311 (2024) **DOI:10.1007/s00170-023-12794-z**.

[108] Cao, L., Guo, W., He, B., Li, W., Huang, X., Zhang, Y., et al. Multi-sensor fusion-based in-situ monitoring of the small changes in process parameters during LPBF. *SSRN* **DOI:10.2139/ssrn.4613005**.

[109] Cao, L., Li, W., Zhang, Y., Cai, W., Wang, Z., Guo, W., et al. Spatter feature-based in-situ identification of disturbances in process parameters during laser powder bed fusion. *Meas Sci Technol 36* 015601 (2025) **DOI:10.1088/1361-6501/ad8022**.

[110] Cao, L., Guo, W., He, B., Li, W., Huang, X., Zhang, Y., et al. In-situ monitoring of the small changes in process parameters with multi-sensor fusion during LPBF. *Meas Sci Technol 35* 106114 (2024) **DOI:10.1088/1361-6501/ad5ea5**.

[111] Zhang, Y., Li, J., Cao, L., Zhou, Q., Cai, W., Yu, L., et al. Two-staged attention-based identification of the porosity with the composite features of spatters during the laser powder bed fusion. *J Manuf Process 131* 2310-2322 (2024) **DOI:10.1016/j.jmapro.2024.10.043**.

[112] Okaro, I.A., Jayasinghe, S., Sutcliffe, C., Black, K., Paoletti, P., Green, P.L. Automatic fault detection for laser powder-bed fusion using semi-supervised machine learning. *Addit Manuf 27* 42-53 (2019) **DOI:10.1016/j.addma.2019.01.006**.

[113] Jayasinghe, J.A.S. *Defect Identification of Laser Powder Bed Fusion Builds Using Photodiode Sensor Readings*. PhD Thesis, University of Liverpool, Liverpool (2022) **DOI:10.17638/03147114**.

[114] Jayasinghe, S., Paoletti, P., Sutcliffe, C., Dardis, J., Jones, N., Green, P.L. Automatic quality assessments of laser powder bed fusion builds from photodiode sensor measurements. *Progr Addit Manuf 7* 143-160 (2022) **DOI:10.1007/s40964-021-00219-w**.

[115] Villalva, G.A.B. Sensor Data Analysis for Additive Manufacturing Process Monitoring. PhD Thesis, University of Liverpool, Liverpool, (2024) **DOI:10.17638/03186294**.

[116] Gutknecht, K., Haferkamp, L., Cloots, M., Wegener, K. Determining process stability of laser powder bed fusion using pyrometry. *Procedia CIRP 95* 127-132 (2020) **DOI:10.1016/j.procir.2020.01.147**.

[117] Gutknecht, K., Cloots, M., Sommerhuber, R., Wegener, K. Mutual comparison of acoustic, pyrometric and thermographic laser powder bed fusion monitoring. *Mater Des 210* 110036 (2021) **DOI:10.1016/j.matdes.2021.110036**.

[118] Kavas, B., Balta, E.C., Tucker, M.R., Krishnadas, R., Rupenyan, A., Lygeros, J., et al. In-situ controller autotuning by Bayesian optimization for closed-loop feedback control of laser powder bed fusion process. *Addit Manuf 99* 104641 (2025) **DOI:10.1016/j.addma.2025.104641**.

[119] Gaikwad, A., Giera, B., Guss, G.M., Forien, J.-B., Matthews, M.J., Rao, P. Heterogeneous sensing and scientific machine learning for quality assurance in laser powder bed fusion-A single-track study. *Addit Manuf 36* 101659 (2020) DOI:10.1016/j.addma.2020.101659.

[120] Forien, J.-B., Calta, N.P., DePond, P.J., Guss, G.M., Roehling, T.T., Matthews, M.J. Detecting keyhole pore defects and monitoring process signatures during laser powder bed fusion: A correlation between in situ pyrometry and ex situ X-ray radiography. *Addit Manuf 35* 101336 (2020) **DOI:10.1016/j.addma.2020.101336**.

[121] Forien, J.-B., Guss, G.M., Khairallah, S.A., Smith, W.L., DePond, P.J., Matthews, M.J., Calta, N.P. Detecting missing struts in metallic micro-lattices using high speed melt pool thermal monitoring. *Addit Manuf Lett 4* 100112 (2023) **DOI:10.1016/j.addlet.2022.100112**.

[122] Gorgannejad, S., Martin, A.A., Nicolino, J.W., Strantza, M., Guss, G.M., Khairallah, S., et al. Localized keyhole pore prediction during laser powder bed fusion via multimodal process monitoring and X-ray radiography. *Addit Manuf 78* 103810 (2023) **DOI:10.1016/j.addma.2023.103810**.

[123] Montazeri, M., Yavari, R., Rao, P., Boulware, P. In-process monitoring of material cross-contamination defects in laser powder bed fusion. *J Manuf Sci Eng 140* 111001 (2018) **DOI:10.1115/1.4040543**.

[124] Yavari, R., Riensche, A., Tekerek, E., Jacquemetton, L., Halliday, H., Vandever, M., et al. Digitally twinned additive manufacturing: Detecting flaws in laser powder bed fusion by combining thermal simulations with in-situ meltpool sensor data. *Mater Des 211* 110167 (2021) **DOI:10.1016/j.matdes.2021.110167**.

[125] King, G. *Prediction of Meltpool Depth in Laser Powder Bed Fusion Using In-Process Sensor Data, Part-level Thermal Simulations, and Machine Learning*, MSc Thesis, University of Nebraska, Lincoln (2022).

[126] Li, X., Li, H., Shen, S., Chen, L., Liu, S., Dai, L., et al. In-situ coaxial temperature monitoring of LPBF melt pool by a compact dual-wavelength thermometry system (CDWTS). *Opt Lasers Eng 194* 109194 (2025) **DOI:10.1016/j.optlaseng.2025.109194**.

[127] Li, X., Li, H., Shen, S., Li, M., Ma, R., Chen, R. et al. In-situ three-dimension monitoring of laser powder bed fusion melt pool and keyhole by binocular imaging. *IEEE Trans Instrum Meas* (2025) **DOI:10.1109/TIM.2025.3608360**.

[128] Lu, X., Chen, Q., Yang, Z., Liu, S., Chen, P., Dong, F. Prediction of porosity in parts using coaxial melt pool imaging and deep learning methods. *Mater Today Commun 45* 112280 (2025) **DOI:10.1016/j.mtcomm.2025.112280**.

[129] Zhou, H., Song, C., Yang, Y., Trofimov, V. In situ monitoring of melt pool and signal modification in laser powder bed fusion. *IEEE Sens J 23* 24944-24953 (2023) **DOI:10.1109/JSEN.2023.3311092**.

[130] Zhou, H., Song, C., Yang, Y., Wang, D., Liu, Z., Xiao, Y., et al. Effect of axial static magnetic field on microstructure evolution, performance, and melt pool signals of AlSi10Mg fabricated by laser powder bed fusion. *Opt Laser Technol 163* 109316 (2023) **DOI:10.1016/j.optlastec.2023.109316**.

[131] Zhou, H., Yang, Y., Trofimov, V., Li, H., Liu, Z., Xiao, Y., et al. In-situ quality monitoring in LPBF via melt-pool radiation: Compressive sampling and deep feature extraction. *Addit Manuf Front 5* 200269 (2026) **DOI:10.1016/j.amf.2025.200269**.

[132] Reijonen, J., Revuelta, A., Riipinen, T., Ruusuvuori, K., Puukko, P. On the effect of shielding gas flow on porosity and melt pool geometry in laser powder bed fusion additive manufacturing. *Addit Manuf 32* 101030 (2020) **DOI:10.1016/j.addma.2019.101030**.

[133] Reijonen, J., Revuelta, A., Nagarajan, H.P.N. Towards data driven quality monitoring: alignment and correlation of photodiode-based co-axial melt pool monitoring signals to part quality in laser powder bed fusion. *IOP Conf Ser Mater Sci Eng 1296* 012009 (2023) **DOI:10.1088/1757-899X/1296/1/012009**.

[134] Reijonen, J., Revuelta, A., Metsä-Kortelainen, S., Salminen, A. Effect of laser focal point position on porosity and melt pool geometry in laser powder bed fusion additive manufacturing. *Addit Manuf 85* 104180 (2024) **DOI:10.1016/j.addma.2024.104180**.

[135] Brandau, B., Mai, T., Brueckner, F., Kaplan, A.F.H. Angular dependence of coaxial and quasi-coaxial monitoring systems for process radiation analysis in laser materials processing. *Opt Lasers Eng 155* 107050 (2022) **DOI:10.1016/j.optlaseng.2022.107050**.

[136] Brandau, B., Brückner, F., Kaplan, A. Proof-Of-Concept of an Absorbance Determination of a Powder Bed by High Resolution Coaxial Multispectral Imaging in Laser Material Processing (2022).

[137] Brandau, B., Brueckner, F., Kaplan, A.F.H. Absorbance determination of a powder bed by high resolution coaxial multispectral imaging in laser powder bed fusion. *Opt Laser Technol 168* 109780 (2024) **DOI:10.1016/j.optlastec.2023.109780**.

[138] Harbig, J., Wenzler, D.L., Baehr, S., Kick, M.K., Merschroth, H., Wimmer, A., Weigold, M., Zaeh, M.F. Methodology to determine melt pool anomalies in powder bed fusion of metals using a laser beam by means of process monitoring and sensor data fusion. *Materials 15* 1265 (2022) **DOI:10.3390/ma15031265**.

[139] Merschroth, H., Harbig, J., Weigold, M., Geis, J., Kirchner, E. Evaluation of Solidification in Powder Bed Fusion Using a High Speed Camera (2022).

[140] Weigold, M., Merschroth, H. Investigation of temperature gradient and solidification rate in laser-based powder bed fusion using a high-speed camera to evaluate local microstructure characteristics. *CIRP Annals 72* 197-200 (2023) **DOI:10.1016/j.cirp.2023.04.031**.

[141] Nadipalli, V.K., Andersen, S.A., Nielsen, J.S., Pedersen, D.B. *Considerations for interpreting in-situ photodiode sensor data in pulsed mode laser powder bed fusion. Joint Special Interest Group Meeting between Euspen and ASPE Advancing Precision in Additive Manufacturing*. The European Society for Precision Engineering and Nanotechnology, 66-69 (2019).

[142] Andersen, S.A., Meinert, K.Æ., Kjer, M.B., Nadimpalli, V.K., Pedersen, D.B. A unified system controller for open-source powder bed fusion systems. *Proceedings of the 33rd Annual International Solid Freeform Fabrication Symposium* 1273-1285 (2022).

[143] Moshiri, M., Pedersen, D.B., Tosello, G., Nadimpalli, V.K. Performance evaluation of in-situ near-infrared melt pool monitoring during laser powder bed fusion. *Virtual Phys Prototyp 18* e2205387 (2023) **DOI:10.1080/17452759.2023.2205387**.

[144] Schwerz, C., Nyborg, L. Linking in situ melt pool monitoring to melt pool size distributions and internal flaws in laser powder bed fusion. *Metals 11* 1856 (2021) **DOI:10.3390/met11111856**.

[145] de Andrade Schwerz, C. *Detection and Classification of Internal Flaws in Laser Powder Bed Fusion: Application of In-situ Monitoring for Quality Control of Hastelloy X Builds*. Chalmers University of Technology, Göteborg (2021).

[146] de Andrade Schwerz, C. In-Situ Monitoring Of Laser Powder Bed Fusion Applied To Defect Detection, Chalmers University of Technology, Göteborg (2023).

[147] Zheng, L., Zhang, Q., Cao, H., Wu, W., Ma, H., Ding, X., et al. Melt pool boundary extraction and its width prediction from infrared images in selective laser melting. *Mater Des 183* 108110 (2019) **DOI:10.1016/j.matdes.2019.108110**.

[148] Zhang, W., Ma, H., Zhang, Q., Fan, S. Prediction of powder bed thickness by spatter detection from coaxial optical images in selective laser melting of 316L stainless steel. *Mater Des 213* 110301 (2022) **DOI:10.1016/j.matdes.2021.110301**.

[149] Zhang, W., Zeng, Y., Wang, J., Ma, H., Zhang, Q., Fan, S. Multi-scale feature pyramid approach for melt track classification in laser powder bed fusion via coaxial high-speed imaging. *Comput Ind 151* 103975 (2023) **DOI:10.1016/j.compind.2023.103975**.

[150] Yadav, P., Rigo, O., Arvieu, C., Le Guen, E., Lacoste, E. Drift detection in selective laser melting (SLM) using a machine learning approach. *International Conference on Additive Manufacturing in Products and Applications* 177-191 (2021) **DOI:10.1007/978-3-030-54334-1_13**.

[151] Yadav, P., Rigo, O., Arvieu, C., Le Guen, E., Lacoste, E. Data treatment of in situ monitoring systems in selective laser melting machines. *Adv Eng Mater 23* 2001327 (2021) **DOI:10.1002/adem.202001327**.

[152] Yadav, P. *Drift Detection in L-PBF Process Using In-Situ Monitoring Instrumentation and Data Analytic Techniques*. University of Bordeaux, Bordeaux (2022).

[153] Wei, W., Li, Y., Wu, H., Li, X., Zhang, Y., Ren, H. et al. GCS-Unet: A lightweight attention network for coaxial melt pool monitoring in laser powder bed fusion. *Smart Mater Manuf 3* 100094 (2025) **DOI:10.1016/j.smmf.2025.100094**.

[154] Zhang, Y., Ren, H., Yan, H., Long, Y. In situ study of surface morphology formation mechanism during laser powder bed fusion. *Appl Sci 15* 2550 (2025) **DOI:10.3390/app15052550**.

[155] Vasileska, E., Tomov, M., Xiaoshuan, Z., Gecevska, V. In-situ optical emission spectroscopy for process monitoring and material identification in laser powder bed fusion. *IEEE International Conference Automatics and Informatics* 608-613 (2024) **DOI:10.1109/ICAI63388.2024.10851538**.

[156] Vasileska, E., Caprio, L., Demir, A.G., Previtali, B., Gecevska, V. Defect classification and dimensional estimation in single-point exposure laser powder bed fusion of lattice struts using optical emission spectroscopy. *Prog Addit Manuf 10* 9177-9193 (2025) **DOI:10.1007/s40964-025-01184-4**.

[157] Snow, Z., Scime, L., Ziabari, A., Fisher, B., Paquit, V. Observation of spatter-induced stochastic lack-of-fusion in laser powder bed fusion using in situ process monitoring. *Addit Manuf 61* 103298 (2023) **DOI:10.1016/j.addma.2022.103298**.

[158] Snow, Z., Scime, L., Ziabari, A., Fisher, B., Paquit, V. *Machine Learning Enabled Sensor Fusion for In-Situ Defect Detection in Laser Powder Bed Fusion*, Oak Ridge National Laboratory, Oak Ridge (2023) **DOI:10.2172/2301610**.

[159] Raj, A., Owen, C., Stegman, B., Abdel-Khalik, H., Zhang, X., Sutherland, J.W. Predicting mechanical properties from co-axial melt pool monitoring signals in laser powder bed fusion. *J Manuf Process 101* 181-194 (2023) **DOI:10.1016/j.jmapro.2023.04.083**.

[160] Raj, A., Huang, D., Stegman, B., Abdel-Khalik, H., Zhang, X., Sutherland, J.W. Modeling spatial variations in co-axial melt pool monitoring signals in laser powder bed fusion. *J Manuf Process 89* 24-38 (2023) **DOI:10.1016/j.jmapro.2022.12.048**.

[161] Maddison, G. *In-Situ Monitoring and Control During Laser Powder Bed Fusion Of Nickel Superalloys*, PhD thesis, University of Sheffield, Sheffield (2022).

[162] Lai, Y., Phan, M.A.L., Zhu, C., Davies, M.M.J., Maddison, G., Hobbs, M.J., et al. In-situ thermal imaging of laser powder bed fusion: Investigating the influence of preheating temperatures on cooling rates and melt pool dynamics. *SSRN* 4516994 (2023) **DOI:10.2139/ssrn.4516994**.

[163] Ma, H., Mao, Z., Feng, W., Yang, Y., Hao, C., Zhou, J. et al. Online in-situ monitoring of melt pool characteristic based on a single high-speed camera in laser powder bed fusion process. *Appl Therm Eng 211* 118515 (2022) **DOI:10.1016/j.applthermaleng.2022.118515**.

[164] Mao, Z., Feng, W., Ma, H., Yang, Y., Zhou, J., Liu, S., et al. Continuous online flaws detection with photodiode signal and melt pool temperature based on deep learning in laser powder bed fusion. *Opt Laser Technol 158* 108877 (2023) **DOI:10.1016/j.optlastec.2022.108877**.

[165] Grünewald, J., Reimann, J., Wudy, K. Influence of ring-shaped beam profiles on spatter characteristics in laser-based powder bed fusion of metals. *J Laser Appl 35* (2023) **DOI:10.2351/7.0001153**.

[166] Lee, H.W. *Convolutional Neural Network based Pore Detection using the Melt Pool Monitoring Data in the Selective Laser Melting Additive Manufacturing Process*, Seoul National University, Seoul (2022).

[167] Lee, K.-H., Lee, H.W., Yun, G.J. A defect detection framework using three-dimensional convolutional neural network (3D-CNN) with in-situ monitoring data in laser powder bed fusion process. *Opt Laser Technol 165* 109571 (2023) **DOI:10.1016/j.optlastec.2023.109571**.

[168] Tyralla, D., Seefeld, T. Thermal based process monitoring for laser powder bed fusion (LPBF). *Adv Mater Res 1161* 123-130 (2021) **DOI:10.4028/www.scientific.net/AMR.1161.123**.

[169] Tyralla, D., Seefeld, T. *Spatially Resolved Temperature Field Measurement in Powder Bed Fusion for online Detection of Porosity* (2023).

[170] Voigt, J., Bock, T., Hilpert, U., Hellmann, R., Moeckel, M. Edge effects in radial porosity profiles from CT measurements and melt pool signal intensities for laser powder bed fusion. *ArXiv* 2201.11483 (2022) **DOI:10.48550/arXiv.2201.11483**.

[171] Voigt, J., Bock, T., Hilpert, U., Hellmann, R., Moeckel, M. Increased relative density and characteristic melt pool Signals at the edge in PBF-LB/M. *Addit Manuf 57* 102798 (2022) **DOI:10.1016/j.addma.2022.102798**.

[172] Luo, S., Ma, X., Xu, J., Li, M., Cao, L. Deep learning based monitoring of spatter behavior by the acoustic signal in selective laser melting. *Sensors 21* 7179 (2021) **DOI:10.3390/s21217179**.

[173] Li, J., Cao, L., Xu, J., Wang, S., Zhou, Q. In situ porosity intelligent classification of selective laser melting based on coaxial monitoring and image processing. Measurement 187 110232 (2022) **DOI:10.1016/j.measurement.2021.110232**.

[174] Xu, Y., Li, T., Cao, X., Tan, Y., Luo, P. Compressive properties of 316L Stainless steel topology-optimized lattice structures fabricated by selective laser melting. *Adv Eng Mater 23* 2000957 (2021) **DOI:10.1002/adem.202000957**.

[175] Xu, Y., Han, G., Huang, G., Li, T., Xia, J., Guo, D. Properties evaluations of topology optimized functionally graded lattice structures fabricated by selective laser melting. *Materials 16* 1700 (2023) **DOI:10.3390/ma16041700**.

[176] Thombansen, U., Gatej, A., Pereira, M. Process observation in fiber laser-based selective laser melting. *Opt Eng 54* 011008 (2015) **DOI:10.1117/1.OE.54.1.011008**.

[177] Duong, E., Masseling, L., Knaak, C., Dionne, P., Megahed, M. Scan path resolved thermal modelling of LPBF. *Addit Manuf Lett 3* 100047 (2022) **DOI:10.1016/j.addlet.2022.100047**.

[178] Kolb, T., Mahr, A., Huber, F., Tremel, J., Schmidt, M. Qualification of channels produced by laser powder bed fusion: Analysis of cleaning methods, flow rate and melt pool monitoring data. *Addit Manuf 25* 430-436 (2019) **DOI:10.1016/j.addma.2018.11.026**.

[179] Kolb, T., Elahi, R., Seeger, J., Soris, M., Scheitler, C., Hentschel, O., et al. Camera signal dependencies within coaxial melt pool monitoring in laser powder bed fusion. *Rapid Prototyp J 26* 100-106 (2020) **DOI:10.1108/RPJ-01-2019-0022**.

[180] Renken, V., Lübbert, L., Blom, H., Von Freyberg, A., Fischer, A. Model assisted closed-loop control strategy for selective laser melting. *Procedia CIRP 74* 659-663 (2018) **DOI:10.1016/j.procir.2018.08.053**.

[181] Renken, V., Von Freyberg, A., Schünemann, K., Pastors, F., Fischer, A. In-process closed-loop control for stabilising the melt pool temperature in selective laser melting. *Progr Addit Manuf 4* 411-421 (2019) **DOI:10.1007/s40964-019-00083-9**.

[182] Alberts, D., Schwarze, D., Witt, G. High speed melt pool & laser power monitoring for selective laser melting (SLM®). *9th International Conference on Photonic Technologies* (2016).

[183] Alberts, D., Schwarze, D., Witt, G. *In Situ Melt Pool Monitoring and the Correlation to Part Density Of Inconel® 718 for Quality Assurance in Selective Laser Melting* (2017) **Handle:2152/89958**.

[184] Thombansen, U., Gatej, A., Pereira, M. Tracking the course of the manufacturing process in selective laser melting. High-Power Laser Materials Processing: Lasers, Beam Delivery, Diagnostics, and Applications III. *SPIE* 158-164 (2014) **DOI:10.1117/12.2040330**.

[185] Chivel, Y., Smurov, I. On-line temperature monitoring in selective laser sintering/melting. *Phys Procedia 5* 515-521 (2010) **DOI:10.1016/j.phpro.2010.08.079**.

[186] Smurov, I., Doubenskaia, M. Temperature monitoring by optical methods in laser processing. *Laser-Assisted Fabrication of Materials*, Springer, Heidelberg 375-422 (2012) **DOI:10.1007/978-3-642-28359-8_9**.

[187] Stajkovic, J., Kahl, M., Kaserer, L., Braun, J., Scheuringer, S., Mayr-Schmölzer, B., et al. Correlating dimensionless enthalpy, pyrometry, and melt pool geometry within the laser powder bed fusion energetic regime: A path to in-situ melt pool control demonstrated on tungsten. *J Manuf Process 141* 1310-1323 (2025) **DOI:10.1016/j.jmapro.2025.03.033**.

[188] Lindecke, P.N.J., del Castillo, J.M.D., Tarhini, H. A universal method for the evaluation of in situ process monitoring systems in the laser powder bed fusion process. *J Manuf Mater Process 9* 359 (2025) **DOI:10.3390/jmmp9110359**.

[189] Hasan, N., Lee, E.-J., Wessman, A., Shafae, M. RAMPSeg: A robust calibration-free image segmentation method for reliable melt pool analysis in laser powder bed fusion. *J Intell Manuf 37* 1-33 (2025) **DOI:10.1007/s10845-025-02726-x**.

[190] Wilkinson, T., Rendell, P., Barba, D., Churchman, C. A spatial statistics framework for detection of build defects in laser powder bed fusion using on-axis photodiode sensors. *Progr Addit Manuf 10* 8065-8085 (2025) **DOI:10.1007/s40964-025-01095-4**.

[191] Hunter, S., Scarbrough, D., Cottrell, S., Eres-Castellanos, A., Adams, D., Clarke, A., Klemm-Toole, J., Squier, J. Real-time single-element-detection structured illumination optical metrology for laser powder bed fusion. *Opt Express 33* 14677-14694 (2025) **DOI:10.1364/OE.555222**.

[192] Booth, B.G., Leroux, S., Verhees, D., Vandecasteele, M., Blanc, C., Bey-Temsamani, A., Philips, W. Hybrid data fusion for low-cost high-speed monitoring in powder bed fusion 3D printing. *IEEE 17th International Conference on Computer and Automation Engineering* 279-286 (2025) **DOI:10.1109/ICCAE64891.2025.10980583**.

[193] Zalameda, J.N., Hocker, S.J.A., Spaeth, P.W., Widener, B. In situ inspection of laser powder bed fusion Ti-6Al-4V additive manufacturing using an infrared sensor. Thermosense: Thermal Infrared Applications XLVII, *SPIE* 149-155 (2025) DOI:10.1117/12.3054069 **DOI:10.1117/12.3054069**

[194] Esmaeilzadeh, R., Jhabvala, J., Schlenger, L., van der Meer, M., Boillat, E., Cayron, C. et al. Toward architected microstructures using advanced laser beam shaping in laser powder bed fusion of Ti-6Al-4V. *Adv Funct Mater 35* 2420427 (2025) **DOI:10.1002/adfm.202420427**.

[195] Liu, Y. *From Photodiode Signals to CT-Quality Porosity Maps: A Deep Learning-Based Image-to-Image Translation Approach for Porosity Prediction in Laser Powder Bed Fusion*, MSc thesis, UNSW, Sydney (2025) **DOI:10.26190/unsworks/31489**.

[196] Hocine, S., Marussi, S., Farndell, A., Ruckh, E., Lambert-Garcia, R., Getley, A.C.M., et al. Physical twin of an industrial quad-laser powder bed fusion machine for high-speed multi-modal sensing measurements. *Mater Des 252* 113767 (2025) **DOI:10.1016/j.matdes.2025.113767**.

[197] Penny, R.W., Kutschke, Z., Hart, A.J. High-fidelity optical monitoring of laser powder bed fusion via aperture division multiplexing. *NPJ Adv Manuf 2* 28 (2025) **DOI:10.1038/s44334-025-00039-8**.

[198] Kirschbaum, N., Wood, N., Kim, C.-E., Tumkur, T.U., Okwudire, C. Vector-level feedforward control of LPBF melt pool area using a physics-based thermal model. *Addit Manuf 112* 104981 (2025) **DOI:10.1016/j.addma.2025.104981**.

[199] Huang, R.-Y., Lu, J.-Q., Cheng, C.-W., Tsai, M.-C., Lee, A.-C. Multi-data-driven model-based control to improve the accuracy of overhang structures in laser powder bed fusion. *Opt Laser Technol 171* 110398 (2024) **DOI:10.1016/j.optlastec.2023.110398**.

[200] Zhou, T., Huang, W., Chen, C. A real-time monitoring method for selective laser melting of TA1 materials based on radiation detection of a molten pool. *Micromachines 15* 570 (2024) **DOI:10.3390/mi15050570**.

[201] Liu, Y., Nose, K., Okugawa, M., Koizumi, Y., Nakano, T. Fabrication and process monitoring of 316L stainless steel by laser powder bed fusion with μ-helix scanning strategy and narrow scanning line intervals. *Mater Trans 64* 1135-1142 (2023) **DOI:10.2320/matertrans.MT-ME2022006**.

[202] Tekerek, E., Perumal, V., Jacquemetton, L., Beckett, D., Halliday, H.S., Wisner, B., et al. On the process of designing material qualification type specimens manufactured using laser powder bed fusion. *Mater Des 229* 111893 (2023) **DOI:10.1016/j.matdes.2023.111893**.

[203] Pfaff, A., Schäffer, S., Jäcklein, M., Balle, F. Measuring the cooling behavior of melt pools in L-PBF by pyrometry. *Materials 16* 3647 (2023) **DOI:10.3390/ma16103647**.

[204] Scheuschner, N., Heinrichsdorff, F., Oster, S., Uhlmann, E., Polte, J., Gordei, A., et al. In-situ monitoring of the laser powder bed fusion process by thermography, optical tomography and melt pool monitoring for defect detection. *Proceedings of the Lasers in Manufacturing Conference* 1-10 (2023).

[205] Blanc, C., Ahar, A., De Grave, K. Reference dataset and benchmark for reconstructing laser parameters from on-axis video in powder bed fusion of bulk stainless steel. *Addit Manuf Lett 7* 100161 (2023) **DOI:10.1016/j.addlet.2023.100161**.

[206] Wang, R., Standfield, B., Dou, C., Law, A.C., Kong, Z.J. Real-time process monitoring and closed-loop control on laser power via a customized laser powder bed fusion platform. *Addit Manuf 66* 103449 (2023) **DOI:10.1016/j.addma.2023.103449**.

[207] Chen, R., Sodhi, M., Imani, M., Khanzadeh, M., Yadollahi, A., Imani, F. Brain-inspired computing for in-process melt pool characterization in additive manufacturing. *CIRP J Manuf Sci Technol 41* 380-390 (2023) **DOI:10.1016/j.cirpj.2022.12.009**.

[208] Surana, A., Lynch, M.E., Nassar, A.R., Ojard, G.C., Fisher, B.A., Corbin, D., et al. Flaw detection in multi-laser powder bed fusion using in situ coaxial multi-spectral sensing and deep learning. *J Manuf Sci Eng 145* 051005 (2023) **DOI:10.1115/1.4056540**.

[209] Felix, S., Ray Majumder, S., Mathews, H.K., Lexa, M., Lipsa, G., Ping, X., Roychowdhury, S., Spears, T. In situ process quality monitoring and defect detection for direct metal laser melting. *Sci Rep 12* 8503 (2022) **DOI:10.1038/s41598-022-12381-4**.

[210] Bakir, Y. *Investigation of SLM process Phenomena by means of In Situ Monitoring Systems* (2022).

[211] Lin, X., Wang, Q., Fuh, J.Y.H., Zhu, K. Motion feature based melt pool monitoring for selective laser melting process. *J Mater Process Technol 303* 117523 (2022) **DOI:10.1016/j.jmatprotec.2022.117523**.

[212] Ikeshoji, T.-T., Yonehara, M., Kato, C., Yanaga, Y., Takeshita, K., Kyogoku, H. Spattering mechanism of laser powder bed fusion additive manufacturing on heterogeneous surfaces. *Sci Rep 12* 20384 (2022) **DOI:10.1038/s41598-022-24828-9**.

[213] Lanigan, E. *Assessing Flaw Detection Capability of Laser Powder Bed Fusion In Situ Monitoring*, MSc thesis, University of Alabama, Huntsville (2022).

[214] Balaraman, R.K., Hussain, S., Ong, J.K., Tan, Q.Y., Tan, U.-X., Raghavan, N. Prediction of part density in additively manufactured maraging steel with supervised machine learning using pyrometer data. *Mater Today Proc 70* 368-375 (2022) **DOI:10.1016/j.matpr.2022.09.271**.

[215] Przyjemski, A. *Development of a Spectroscopic Process Monitoring System For Multi-Laser Metal Powder Bed Fusion Additive Manufacturing*, MSc thesis, Penn State University, Pennsylvania (2021).

[216] O'Loughlin, S., Dutton, B., Semaj, G., Snell, E., Rindler, J., Groeber, M.A. Towards in-process prediction of voids in laser powder bed fusion. *JOM 73* 3240-3249 (2021) **DOI:10.1007/s11837-021-04885-7**.

[217] Slodczyk, M., Ilin, A., Kiedrowski, T., Bareth, T., Ploshikhin, V. Spatter reduction by multi-beam illumination in laser powder-bed fusion. *Mater Des 212* 110206 (2021) **DOI:10.1016/j.matdes.2021.110206**.

[218] Klein, J., Jaretzki, M., Schwarzenberger, M., Ihlenfeldt, S., Drossel, W.-G. Automated porosity assessment of parts produced by laser powder bed fusion using convolutional neural networks. *Procedia CIRP 104* 1434-1439 (2021) **DOI:10.1016/j.procir.2021.11.242**.

[219] Remani, A., Williams, R., Thompson, A., Dardis, J., Jones, N., Hooper, P., et al. Design of a multi-sensor measurement system for in-situ defect identification in metal additive manufacturing. *Proceedings ASPE/Euspen Advancing Precision in Additive Manufacturing* (2021).

[220] Dursun, G., Pehlivanogullari, B., Sen, C., Orhangul, A. An investigation upon overhang zones by using finite element modelling and in-situ monitoring systems. *Procedia CIRP 93* 1253-1258 (2020) **DOI:10.1016/j.procir.2020.04.118**.

[221] Fernandez, A.G., Tarhini, H., Grottker, S.T., Emmelmann, C. In-situ quality assurance of surface roughness using an on-axis photodiode. *Fraunhofer Direct Digital Manufacturing Conference* 032059 (2020).

[222] Artzt, K., Siggel, M., Kleinert, J., Riccius, J., Requena, G., Haubrich, J. Pyrometric-based melt pool monitoring study of CuCr1Zr processed using L-PBF. *Materials 13* 4626 (2020) **DOI:10.3390/ma13204626**.
[223] Mohr, G., Altenburg, S.J., Ulbricht, A., Heinrich, P., Baum, D., Maierhofer, C., et al. In-situ defect detection in laser powder bed fusion by using thermography and optical tomography-comparison to computed tomography. *Metals 10* 103 (2020) **DOI:10.3390/met10010103**.
[224] Francis, Z.R., Chong, T., Ginn Jon, S., Hai, D., Lars, J., Scott, B. et al. Combination of Modeling and Thermal Sensing to Understand Additive Manufacturing Processes, White Paper (2019).
[225] Fisher, B.A., Beuth, J. *Part Temperature Effects in Powder Bed Fusion Additive Manufacturing of Ti-6Al-4V*, PhD thesis, Carnegie Mellon University, Pittsburgh, (2018) **DOI:10.1184/R1/6720995**.
[226] Liu, C., Chen, Z., Cao, H., Zhou, J. Coaxial monitoring of temperature field in selective pulsed laser melting. *Proc SPIE* 104573G (2017) **DOI:10.1117/12.2286275**.
[227] Kanko, J.A., Sibley, A.P., Fraser, J.M. In situ morphology-based defect detection of selective laser melting through inline coherent imaging. *J Mater Process Technol 231* 488-500 (2016) **DOI:10.1016/j.jmatprotec.2015.12.024**.
[228] Jamshidinia, M., Boulware, P., Marchal, J., Mendoza, H., Cronley, L., Kelly, S., et al. In-process monitoring of cross contamination in laser powder bed fusion (L-PBF) additive manufacturing (AM). *International Solid Freeform Fabrication Symposium* (2016).
[229] Chivel, Y. Optical monitoring and control of the surface thermal processes. European Congress and Exhibition on Powder Metallurgy. *European PM Conference Proceedings* (2016).
[230] Van Gestel, C. Study of physical phenomena of selective laser melting towards increased productivity, *EPFL* (2015) **DOI:10.5075/epfl-thesis-6817**.
[231] Rombouts, M., Kruth, J.-P., Froyen, L., Mercelis, P., Fundamentals of selective laser melting of alloyed steel powders. *CIRP Annals 55* 187-192 (2006) **DOI:10.1016/S0007-8506(07)60395-3**.
[232] Bidare, P. *An Open-Architecture Laser Powder Bed Fusion System and Its Use for In-Situ Process Measurements*, Heriot-Watt University (2018).
[233] Andreau, O., Koutiri, I., Peyre, P., Penot, J.-D., Saintier, N., Pessard, E., et al. Texture control of 316L parts by modulation of the melt pool morphology in selective laser melting. *J Mater Process Technol 264* 21-31 (2019) **DOI:10.1016/j.jmatprotec.2018.08.049**.
[234] Reijonen, J. Effect of laser parameters and shielding gas flow on co-axial photodiode-based melt pool monitoring signals in laser powder bed fusion. *Addit Manuf Lett 11* 100244 (2024) **DOI:10.1016/j.addlet.2024.100244**.
[235] Poyraz, O., Kuşhan, M. Residual stress-induced distortions in laser powder bed additive manufacturing of nickel-based superalloys. *Stroj Vestn-J Mech Eng 65* 343-350 (2019) **DOI:10.5545/sv-jme.2019.6004**.
[236] König, H.-G., Pütsch, O., Stollenwerk, J., Loosen, P. An improved approach for process monitoring in laser material processing. *Optical Modelling and Design IV, SPIE* 133-138 (2016) **DOI:10.1117/12.2223779**.

Acknowledgements *This work was funded by the Slovenian Research and Innovation Agency (P2-0270 and P2-0241) and by the European Union (ERC, MeltingWell, 101219492). Views and opinions expressed are however those of the authors only and do not necessarily reflect those of the European Union or the European Research Council. Neither the European Union nor the granting authority can be held responsible for them.*

Received *2026-06-09,* **revised** *2026-09-29,* **accepted** *2026-10-21 as Review Scientific Paper.*

Data availability *The data supporting the findings of this study are included in the article and/or its supplementary materials.*

Author contribution *Dominik Kozjek: Conceptualization, Methodology, Software, Validation, Formal analysis, Investigation, Resources, Data Curation, Writing - Original Draft, Writing - Review & Editing, Visualization, Supervision, Project administration, Funding acquisition; Drago Bračun: Methodology, Software, Validation, Formal analysis, Investigation, Resources, Writing - Review & Editing; Andrej Jeromen: Validation, Investigation, Writing - Review & Editing; Fred M. Carter III: Validation, Investigation, Resources, Writing - Review & Editing; Primož Podržaj: Resources, Writing - Review & Editing, Supervision, Funding acquisition; Edvard Govekar: Resources, Data Curation, Writing - Review & Editing, Supervision, Funding acquisition*

AI-Assisted writing *During the preparation of this manuscript, the authors used AI-assisted tools solely for language editing, including improvements in grammar, spelling, clarity, readability, and academic writing style. AI tools were not used for generating scientific ideas, developing hypotheses, conducting analyses, interpreting or validating results, or drawing scientific conclusions. All scientific content was developed and critically reviewed by the authors, who take full responsibility for the accuracy, originality, and integrity of the manuscript.*

Soosno spremljanje talilnega bazena za krmiljenje procesa selektivnega laserskega taljenja

Povzetek *Zanesljivo spremljanje procesa je ključnega pomena za nadaljnji razvoj selektivnega laserskega taljenja (SLM), saj zagotavlja procesne informacije, potrebne za izvajanje korektivnih krmilnih ukrepov za preprečevanje napak, kot sta nezadostno zlitje materiala in poroznost zaradi nastanka parnega kanala. Obetaven pristop k spremljanju procesa SLM je soosno merjenje svetlobe, ki jo oddaja območje talilnega bazena. Doslej je bilo izvedenih več kot dvesto raziskav soosnega spremljanja talilnega bazena, vendar še vedno ni validirane in zanesljive metode za merjenje ustrezne veličine, ki bi jo bilo mogoče neposredno uporabiti kot vhodni podatek za visokoločljivostno krmiljenje procesa SLM. Takšno krmiljenje bi omogočalo dinamično prilagajanje procesnih parametrov, kot sta moč laserja in hitrost skeniranja, ne le na ravni celotnega izdelka, temveč tudi lokalno, za posamezne mikrometrske odseke vzdolž poti skeniranja. V prispevku so pregledane obstoječe raziskave soosnega spremljanja talilnega bazena ter opredeljene možne smeri prihodnjih raziskav in razvoja za vzpostavitev standardizirane in zanesljive metode spremljanja talilnega bazena. Kot posebej obetavna veličina za krmiljenje procesa je prepoznana globina talilnega bazena. Z možnostjo spremljanja in regulacije globine talilnega bazena bi se bilo mogoče izogniti neustreznim procesnim pogojem zaradi prevelikega ali premajhnega vnosa energije, ki povzročajo napake, kot sta poroznost zaradi nastanka parnega kanala in nezadostno zlitje materiala. Vendar je bilo v objavljeni znanstveni literaturi predstavljenih le pet raziskav, v katerih so avtorji poskušali soosno oceniti globino talilnega bazena med procesom SLM. Kljub tem poskusom še vedno ni dovolj validirane metode za visokoločljivostno soosno spremljanje globine talilnega bazena pri procesu SLM. Potencialna rešitev se kaže v združevanju konceptov in najnovejših spoznanj s področja dvobarvnega soosnega spremljanja območja talilnega bazena s kamerami in fotodiodami. Na podlagi obstoječe literature in praktičnih izkušenj z vzpostavljanjem ter uporabo sistemov za soosno spremljanje prispevek podaja tudi smernice in izpostavlja najpogostejše izzive pri vzpostavitvi soosnega spremljanja talilnega bazena v procesu SLM.*

Ključne besede *proces PBF-LB/M, selektivno lasersko taljenje (SLM), soosno spremljanje, talilni bazen, emisija svetlobe, valovna dolžina, pregledni članek*